UNITED NATIONS EDUCATIONAL, SCIENTIFIC AND CULTURAL ORGANIZATION
INTERNATIONAL ATOMIC ENERGY AGENCY
INTERNATIONAL CENTRE FOR THEORETICAL PHYSICS
I.C.T.P., P.O. BOX 586, 34100 TRIESTE, ITALY, CABLE: CENTRATOM TRIESTE

H4.SMR/1058-9

WINTER COLLEGE ON OPTICS

9 - 27 February 1998

Physical Properties and Applications of Photorefractive Materials

Y. Tomita

Department of Electronics Engineering, University of Electro-Communications, Tokyo, Japan

International Centre for Theoretical Physics
Winter College on Optics
11-13 February 1998
Trieste Italy

Physical Properties and Applications of Photorefractive Materials

Yasuo Tomita

Department of Electronics Engineering
University of Electro-Communications
1-5-1 Chofugaoka, Chofu, Tokyo 182, Japan
Fax: +81(424)80-3801
Email: ytomita@ee.uec.ac.jp

International Centre for Theoretical Physics
Winter College on Optics
11-13 February 1988

Physical Properties and Applications of Photorefractive Materials

YASUO TOMITA

UNIVERSITY OF ELECTRO-COMMUNICATIONS
TOKYO, JAPAN

OUTLINE

- Introduction to Nonlinear Optics
- The Photorefractive Effect
- Two- and Four-Wave Mixing
- Self- and Mutually-Pumped Phase Conjugators
- Photorefractive Materials
- Applications

REFERENCES

Books

1. P. Günter and J.-P. Huignard, Eds., "Photorefractive Materials and Their Applications I and II," (Springer-Verlag, 1988).
2. P. Yeh, "Introduction to Photorefractive Nonlinear Optics," (Wiley, 1993).
3. D.D. Nolte, Ed., "Photorefractive Effects and Materials," (Kluwer Academic Publishers, 1995).
4. L. Solymer *et al.*, "The Physics and Applications of Photorefractive Materials," (Oxford, 1996).
5. P. Yeh and C. Gu, Eds., "Landmark Papers on Photorefractive Nonlinear Optics," (World Scientific, 1995).
6. M. Cronin-Golomb and M. Klein, M. Bass, Ed., "Handbook of Optics," chap. 39, (McGraw-Hill, 1995).
7. A. Yariv, "Optical Electronics in Modern Communications," chap. 18, (Oxford, 1997).

Review articles

(general reviews)

1. P. Günter, Phys. Rep. **93**, 201-299 (1982).
2. T.J. Hall *et al.*, Prog. Quantum Electron. **10**, 77-146 (1985).
3. J. Feinberg, Physics Today **41**, 46-52 (1988).
4. D.M. Peper *et al.*, Sci. Am. **263**(4), 34-40 (1990).

(photorefractive materials)

1. G.C. Valley *et al.*, Ann. Rev. Mater. Sci. **18**, 165-188 (1988).
2. A.M. Glass, Opt. Quantum Electron. **22**, S1-S16 (1990).
3. W.E. Moerner and S.M. Silence, Chem. Rev. **94**, 127-155 (1994).
4. B. Kippelen et al., H.S. Nalwa and S. Miyata Eds., "Nonlinear Optics of Organic Molecules and Polymers," chap.8, (CRC Press, New York, 1996).

(photorefractive wave mixing, oscillation and phase conjugation)

1. P.Yeh, IEEE J. Quantum Electron. QE-**25**, 484-519 (1989).
2. S.-K. Kwong *et al.*, IEEE J. Quantum Electron. QE-**22**,1508-1523 (1986).
3. Y. Tomita *et al.*, IEEE J. Quantum Electron. QE-**25**, 315-338 (1989).
4. B. Fischer *et al.*, IEEE J. Quantum Electron. QE-**25**, 550-569 (1989).
5. P. Yeh, Proc. IEEE **80**, 436-450 (1992).
6. L. Solymer *et al.*, Prog. Quantum Electron. **18**, 377-450 (1994).
7. B.I. Sturman *et al.*, Phys. Rep. **275**, 197-254 (1996).

(applications to optical information processing)

1. D.Z. Anderson and J. Feinberg, IEEE J. Quantum Electron. QE-**25**, 635-647 (1989).
2. Y. Owechko, IEEE J. Quantum Electron. QE-**25**, 619-634 (1989).
3. P. Yeh et al., Opt. Eng. **28**, 328-343 (1989).
4. L.-J. Cheng *et al.*, Int. J. Opt. Comput. **2**, 111-142 (1991).
5. F.T.S. Yu and S.Yin, Int. J. Opt. Comput. **2**, 143-164 (1991).
6. J. Hong, Opt. Quantum Electron. **25**, S551-S568 (1993).
7. L. Hesselink and M.C. Bashow, Opt. Quantum Electron. **25**, S611-S661 (1993).
8. D. Psaltis and F. Mok, Sci. Am. **273**, 70-76 (1995).

Introduction to Nonlinear Optics

Induced polarization in a medium

$$\mathbf{P} = \varepsilon_0 \chi_{\text{linear}}\,\mathbf{E} + \varepsilon_0 \chi^{(2)}\,\mathbf{EE} + \varepsilon_0 \chi^{(3)}\,\mathbf{EEE} + \cdots$$
$$= \varepsilon_0 \chi_{\text{linear}}\,\mathbf{E} + \varepsilon_0 \left(\chi^{(2)}\mathbf{E} + \chi^{(3)}\,\mathbf{EE} + \cdots\right)\mathbf{E}$$
$$= \varepsilon_0 \chi_{\text{linear}}\,\mathbf{E} + \varepsilon_0 \chi_{\text{nonlinear}}(\mathbf{E})\mathbf{E}$$

where

$$\chi_{\text{linear}} = n_b^2 - 1$$
$$\chi_{\text{nonlinear}}(\mathbf{E}) = 2n_b \Delta n(\mathbf{E}) + (\Delta n(\mathbf{E}))^2 \approx 2n_b \Delta n(\mathbf{E})$$

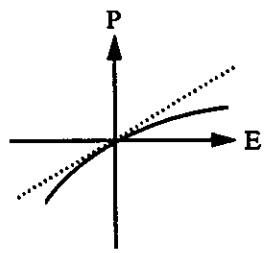

Pockels (linear electrooptic) effect

$$n = n_b + \Delta n(\mathbf{E}) = n_b - \frac{1}{2} n_b^3 r E^{\Omega(<<\omega)}$$

Optical Kerr effect

$$n = n_b + \Delta n(\mathbf{E}) = n_b + n_2 I$$

Photorefractive effect

$$n = n_b - \frac{1}{2} n_b^3 r E_{sc}$$
$$= n_b - \frac{1}{2} n_b^3 r E_{sc}^0 \left[\frac{2E_1^\omega \left(E_2^\omega\right)^*}{I}\right]$$

Nonlinear Refraction: a comparison

Optical Kerr effect

i) nonresonant case

$n_2 \approx 3 \times 10^{-16}\ \text{cm}^2/\text{W}$ for glass (silica)

ii) resonant case (exciton saturation)

$n_2 \approx 2 \times 10^{-5}\ \text{cm}^2/\text{W}$ for bulk GaAs at 300K

$4 \times 10^{-3}\ \text{cm}^2/\text{W}$ for AlGaAs/GaAs MQWs

Photorefractive effect

$\Delta n/I \approx 1 \times 10^{-5} \sim 1 \times 10^{-4}\ \text{cm}^2/\text{W}$ for typical bulk materials

$\sim 1 \times 10^{-3}\ \text{cm}^2/\text{W}$ for some PR polymers

The Photorefractive Effect

The Photorefractive Effect

– charge-transport optical nonlinearity–

Discovered as "optical damage" in $LiNbO_3$ and $LiTaO_3$

[A.Ashkin *et al.*, Appl.Phys.Lett. **9**, 72-74 (1966)]

Advantages

- large (nonlocal) nonlinearity with low-intensity cw light
- long interaction length possible due to low absorption
- broadband sensitivity

Disadvantages

- slow response speed ($\propto$ intensity)
- bulky sample size

Requirements for being *photorefractive*

- electrooptic
- photoconductive
- low dark-conductive

The Photorefractive Effect

– mechanism–

Fundamental processes for the photorefractive effect
- photoexcitation of carriers
- charge transport

[– charge trapping]
- space-charge field formation
- refractive index changes via the electrooptic effect

This charge migration results in setting up high electric fields in a crysal on the order of kV/cm or even more !

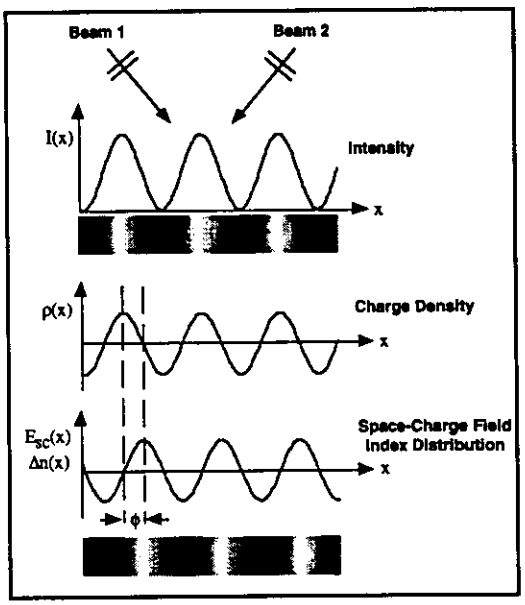

Band-Transport Model

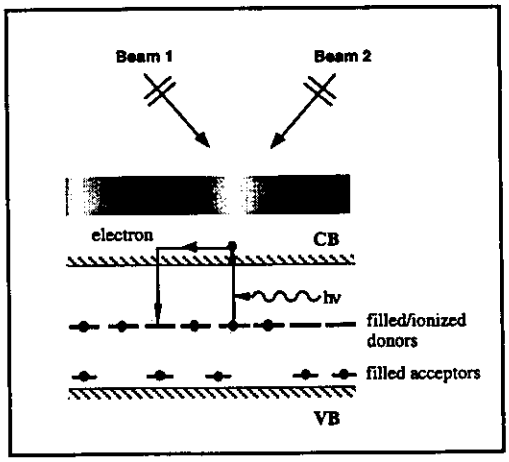

Mechanisms responsible for transporting carriers

i) diffusion

$j_{diff}=DeVn$

where

$D=\mu k_B T/|e|$

ii) drift

$j_{drift}=\sigma E$

where

$\sigma=|e|\mu n$

and

$E=E_{sc}+E_0$

iii) bulk photovoltaic effect

$(j_{ph})_i=(\beta_{ijk}E_j^{*}E_k+c.c.)/2$

Band-Transport Equations

[N.V.Kukhtarev *et al.*, Ferroelectrics 22, 949-964 (1979)]

$$\frac{\partial N^+}{\partial t} = (\beta + sI)(N - N^+) - \gamma_R n N^+ \qquad \text{(rate equation)}$$

$$\frac{\partial N^+}{\partial t} = \frac{\partial n}{\partial t} - \frac{1}{e}\nabla \cdot \mathbf{j} \qquad \text{(continuity equation)}$$

$$\mathbf{j} = \mathbf{j}_{diff} + \mathbf{j}_{drift} + \mathbf{j}_{ph}$$

$$\nabla \cdot (\varepsilon \mathbf{E}) = e(N^+ - N_A^- - n) \qquad \text{(Poisson's equation)}$$

where $\mathbf{E} = \mathbf{E}_{sc} + \mathbf{E}_0$

N = total donor density
N^+ = ionized donor density
N_A^- = ionized acceptor density
n = electron density
β = dark (thermal) generation rate
s = photoionization cross section
γ_R = recombination coefficient

Linearization and Approximations

(Linearization)

Consider the solution in the following form:

$$F(z,t) = F_0(t) + F_1(z,t)$$
$$= F_0(t) + \frac{1}{2}F_1(t)\exp(-iKz) + \text{c.c.}$$

Neglect the 2nd-order terms such as

$$nN^+ = n_0N_0^+ + n_0N_1^+ + n_1N_0^+ + n_1N_1^+$$
$$\approx n_0N_0^+ + n_0N_1^+ + n_1N_0^+$$

(Approximations)

$$n_0 << N_A^- \quad (\text{low} - \text{intensity excitation})$$

$$\frac{\partial n_0}{\partial t} = 0 \quad (\text{quasi} - \text{steady approximation})$$

Solution to Linearized Equations

For the intensity interference patterns

$$I(z) = I_0 + \frac{1}{2} I_1 \exp(-iKz) + \text{c.c.} = I_0\left[1 + \frac{1}{2} m \exp(-iKz) + \text{c.c.}\right]$$

the transient solution of the space-charge field is given by

$$E_{sc}(z,t) = E_0 + \frac{1}{2}|E_{sc1}| e^{i\phi}\left(1 - e^{-t/\tau + i\omega_g t}\right) e^{-iKz} + \text{c.c.} \qquad (m \ll 1)$$

where

$$|E_{sc1}| = \frac{m}{1+\beta/sI_0} E_q \left[\frac{(E_0 - E_{ph})^2 + E_d^2}{E_0^2 + (E_d + E_q)^2}\right]^{1/2}$$

$$\phi = \tan^{-1}\left[\frac{(E_d + E_q)E_d + E_d(E_0 - E_{ph})}{E_q(E_0 - E_{ph}) - E_d E_{ph}}\right]$$

$$\tau = \tau_{di} \frac{(1 + E_d/E_\mu)^2 + (E_0/E_\mu)^2}{(1 + E_d/E_q)(1 + E_d/E_\mu) + E_0^2/E_q E_\mu}$$

$$\omega_g = \frac{1}{\tau_{di}} \frac{E_0/E_q - E_0/E_\mu}{(1 + E_d/E_\mu)^2 + (E_0/E_\mu)^2}$$

(diffusion field) (saturation field)

$$E_d = k_B TK/e, \quad E_q = eN_{eff}/\varepsilon K$$

(mobility field)

$$E_\mu = \gamma_R N_A^- / \mu K$$

(photovoltaic field)

$$E_{ph} = p\gamma_R N_A^- / e\mu s$$

(dielectric relaxation time)

$$\tau_{di} = \varepsilon / e\mu n_0$$

(effective trap density)

$$N_{eff} = N_A^-(N - N_A^-)/N$$

Steady-State Space-Charge Field – diffusion operation ($E_0 = 0$) –

$$|E_{sc1}| = \frac{m}{1+\beta/sI_0} \frac{E_q E_d}{E_d + E_q}$$

$$\rightarrow |E_{sc1}|_{max} = \frac{m}{1+\beta/sI_0} \frac{1}{2}\left(\frac{k_B T N_{eff}}{\varepsilon}\right)^{1/2} \text{ when } E_d = E_q \left[\text{i.e., } \Lambda = \Lambda_{Debye} = \frac{2\pi}{e}\left(\frac{k_B T \varepsilon}{N_{eff}}\right)^{1/2}\right]$$

$$\phi = \frac{\pi}{2}$$

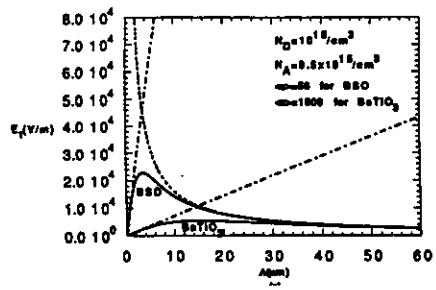

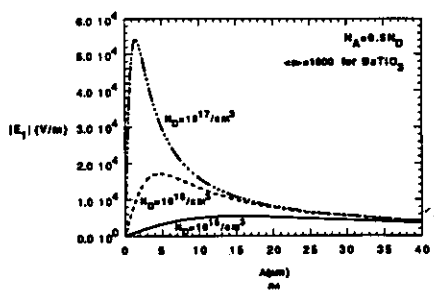

P.Yeh, Introduction to PR NLO(1993)

Steady-State Space-Charge Field
– drift operation ($E_0 \neq 0$) –

$$|E_{sc1}| = \frac{m}{1+\beta/sI_0}\left(\frac{E_q E_d}{E_d + E_q}\right)\left[\frac{1+(E_0/E_d)^2}{1+(E_0/(E_d+E_q))^2}\right]^{1/2}$$

$$\phi \neq \frac{\pi}{2} \quad \text{but } \phi \to \frac{\pi}{2} \text{ when } E_0 >> E_d, E_q$$

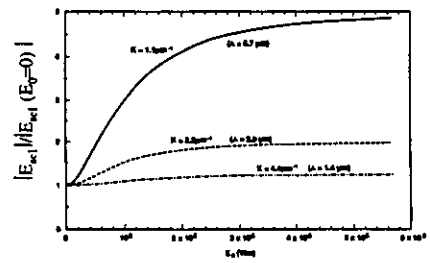

P.Yeh, Introduction to PR NLO(1993)

Space-Charge Field
– transient behavior –

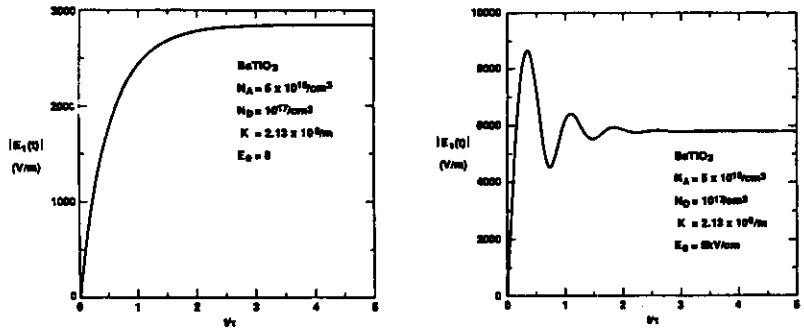

P.Yeh, Introduction to PR NLO(1993)

Effective Electrooptic Coefficient

The electrooptic effect is formally defined as a change in the optical impermeability tensor $\tilde{\eta}(\equiv \varepsilon_0 \tilde{\varepsilon}^{-1})$

$$\begin{aligned}\Delta\tilde{\eta}_{ij} &\equiv \tilde{\eta}_{ij}(E^{\Omega}) - \tilde{\eta}_{ij}(0) \\ &= \varepsilon_0\left[\tilde{\varepsilon}(E^{\Omega})^{-1}\right]_{ij} - \varepsilon_0\left[\tilde{\varepsilon}(0)^{-1}\right]_{ij} \\ &= -\varepsilon_0\left[\tilde{\varepsilon}^{-1} : \Delta\tilde{\varepsilon} : \tilde{\varepsilon}^{-1}\right]_{ij} \\ &= \tilde{r}_{ijk}E_k^{\Omega} + \tilde{s}_{ijkl}E_k^{\Omega}E_l^{\Omega}\end{aligned}$$

For the first-order electrooptic (Pockels) effect

$$\Delta\tilde{\varepsilon} = -\varepsilon_0^{-1}E^{\Omega}\left[\tilde{\varepsilon} : (\tilde{r} : e_E) : \tilde{\varepsilon}\right]$$

Photorefractive refractive index grating formed by two-beam interference

$$\Delta\tilde{n} \approx \frac{1}{2\varepsilon_0 n}\left(e_1^* : \Delta\tilde{\varepsilon} : e_2\right)$$

$$\equiv -\frac{1}{2}n^3\tilde{r}_{eff}E_{sc}$$

where

$$n = n_e n_o\left[n_e^2\sin^2\theta + n_o^2\cos^2\theta\right]^{1/2}$$

For 4mm symmetry crystals (e.g., $BaTiO_3$ and SBN)

$$r_{eff} = r_{13}\cos\beta \qquad \text{for s-polarized beams}$$

$$r_{eff} = \{n_e^4 r_{33}\cos(\beta-\theta)\cos(\beta+\theta) + 2n_e^2 n_o^2 r_{42}\sin^2\beta + n_o^4 r_{13}\sin(\beta-\theta)\sin(\beta+\theta)\}\left(\cos\beta/n^4\right)$$

for p-polarized beams

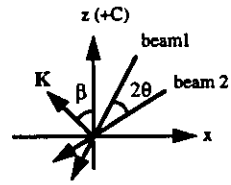

Effective Electrooptic Coefficient

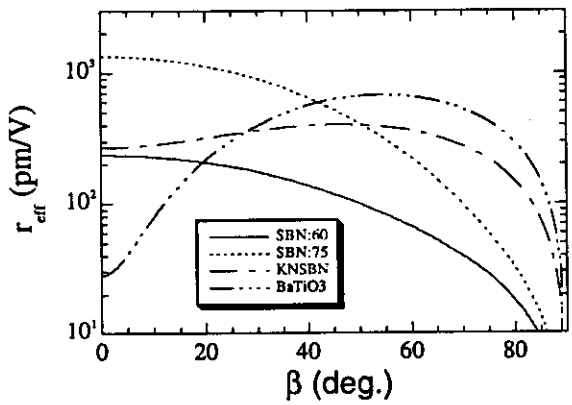

Photorefractive Two-Wave Mixing

Two-Wave Mixing

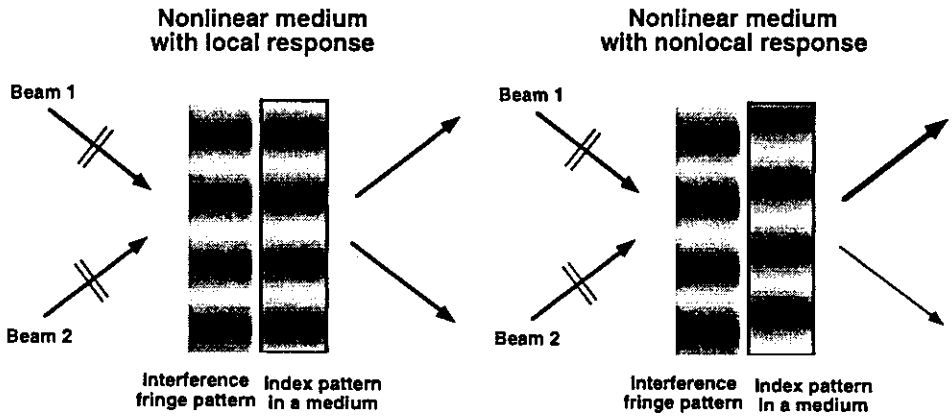

Diffraction Properties in Two-Wave Mixing

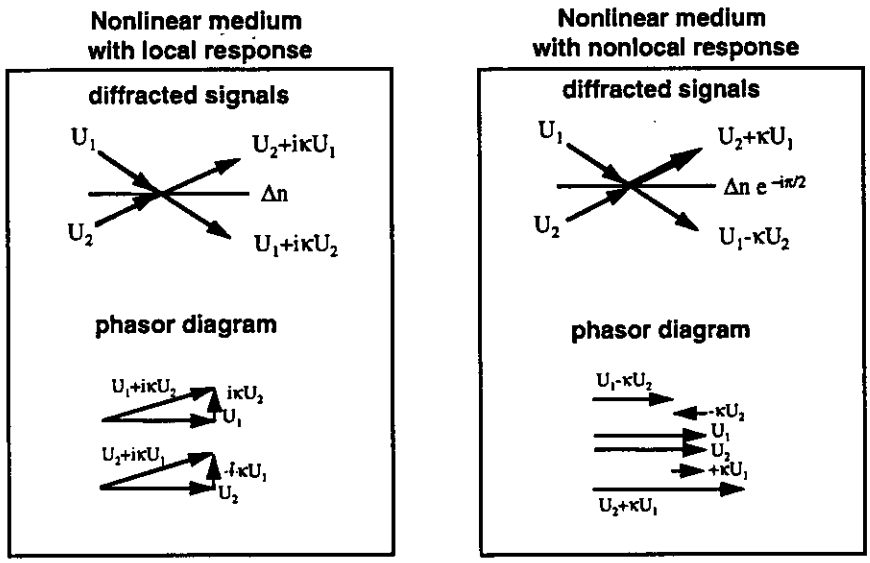

Two-Beam Coupling in a Photorefractive Medium

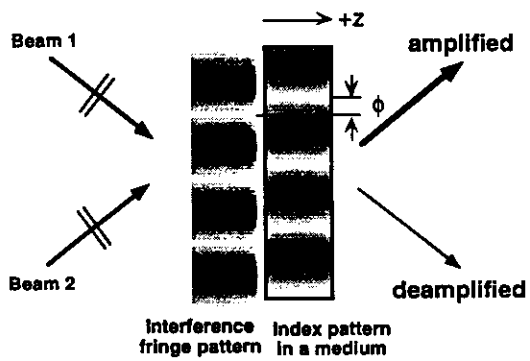

$$\frac{dI_1}{dz} = -\alpha I_1 - 2\gamma' \frac{I_1 I_2}{I_1 + I_2}$$

$$\frac{dI_2}{dz} = -\alpha I_2 + 2\gamma' \frac{I_1 I_2}{I_1 + I_2}$$

$$\frac{d(\varphi_1 - \varphi_2)}{dz} = \gamma'' \frac{I_1 - I_2}{I_1 + I_2}$$

where

$$\gamma' = \frac{2\pi n_1}{\lambda \cos\theta} \sin\phi$$

$$\gamma'' = \frac{\pi n_1}{\lambda \cos\theta} \cos\phi$$

$$n_1 = -\frac{1}{2m} n^3 r_{eff} |E_{sc1}|$$

Note that ϕ is determined by the crystal's orientation and the sign of carriers.

Two-Beam Coupling in a Photorefractive Medium

General solutions

$$I_1(z) = \frac{\beta I_0}{\beta + \exp(\Gamma z)} \exp(-\alpha z)$$

$$I_2(z) = \frac{I_0}{1 + \beta \exp(-\Gamma z)} \exp(-\alpha z)$$

$$\Delta\varphi(z) = \Delta\varphi(0) + \frac{1}{2}\cot\phi \ln\left\{\frac{(1+\beta)^2 \exp(-\Gamma z)}{[\beta + \exp(-\Gamma z)]^2}\right\}$$

where

$$I_0 = I_1(0) + I_2(0)$$

$$\beta = \frac{I_1(0)}{I_2(0)}$$

$\Gamma = 2\gamma'$ = exponential coupling gain coefficient

Important properties

i) $|\phi| = \pi/2$ (diffusion operation)
- *maximum* nonreciprocal energy transfer
- *no* phase crosstalk

ii) $0 \le |\phi| < \pi/2$ (drift operation)
- noreciprocal energy transfer for $\phi \neq 0$
- phase crosstalk

Limiting cases

i) $\phi \neq 0$ and $\beta \exp(-\Gamma z) >> 1$

$$I_2(z) \approx I_2(0) \exp[(\Gamma - \alpha)z]$$

ii) $\phi = 0$

$$\Delta\varphi(z) = \Delta\varphi(0) + \frac{1-\beta}{1+\beta}\frac{\Gamma z}{2}$$

iii) $\beta >> 1$

$$\Delta\varphi(z) = \Delta\varphi(0) - \frac{1}{2}\Gamma z \cot\phi$$

Numerical Examples

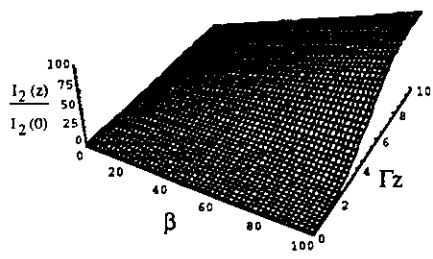

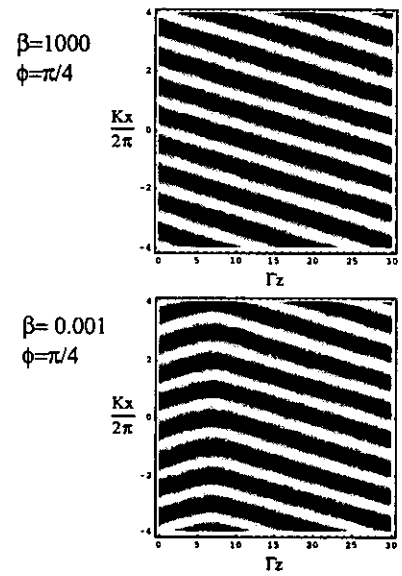

Photorefractive Response Time (τ) vs. Two-Beam Coupling Buildup Time (τ_{2bc})

Determination of τ is important for estimating photorefractive parameters such as $\mu\tau_R$.
But the 2WM buildup time τ_{2bc} is usually different from τ.

Relationship between τ and τ_{2bc} for $\beta >> 1$

$$\tau_{2bc} \approx \begin{cases} \tau\{1+0.41\Gamma L+0.074(\Gamma L)^2+O[(\Gamma L)^3]\}, \\ \text{for } \Gamma L < 2.2 \\ \tau\dfrac{\Gamma L}{2}\{1+[(1-1/e)^{1/2}-1/2](8\pi/\Gamma L)^{1/2} \\ +O[(1/\Gamma L)]\}, \quad \text{for } \Gamma L > 2.2 \end{cases}$$

(Vachss, 1990)

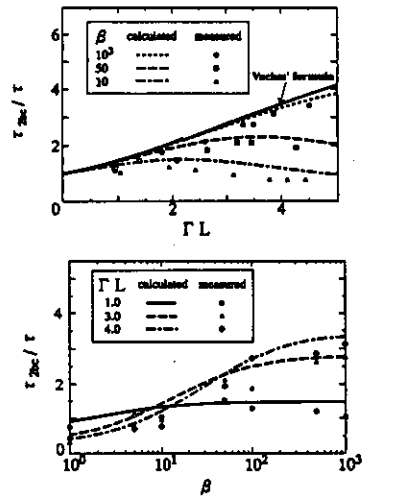

Matsushima and Tomita, Opt. Commun. 128, 287 (1996)

Experimental Setup

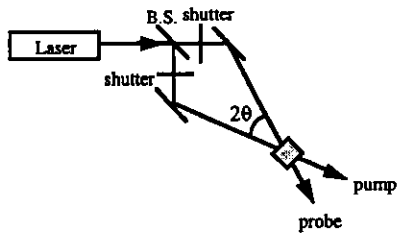

Theoretical gain coefficient

$$\Gamma = \frac{1}{1+I_s/I}\left(\frac{A\sin\theta}{1+B^{-2}\sin^2\theta}\right)\left(\frac{\cos 2\theta'}{\cos\theta'}\right)$$

where

$I_s \propto \beta_{dr}/s$
$A \propto r_{eff}$
$B^2 \propto N_{eff}$

Measured gain coefficient

$$g = \frac{I_{probe}\ (w/\ pump)}{I_{probe}\ (w/o\ pump)}$$

$$\Rightarrow \Gamma = \frac{1}{L}\ln\left(\frac{g\beta}{1+\beta-g}\right)$$

Response rate

$$\tau^{-1} = \frac{1}{\varepsilon_0\varepsilon_s}(\sigma_{dark} + e\lambda\alpha\mu\tau_R I/hc) \times\left[1+(2\pi L_D/\Lambda)^2\right]$$

Experimental Results
– $Sr_{0.6}Ba_{0.4}Nb_2O_6$:Cr (Cr-doped SBN:60)–

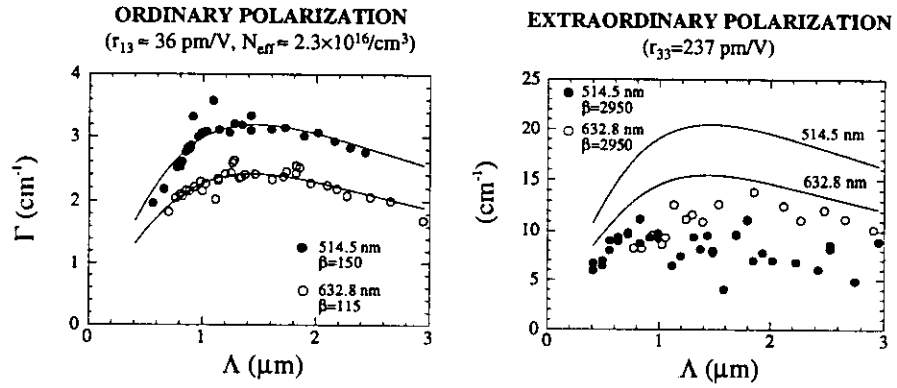

Tomita and Suzuki, Appl. Phys. A **59**, 579 (1994)

Angular Dependence of Γ

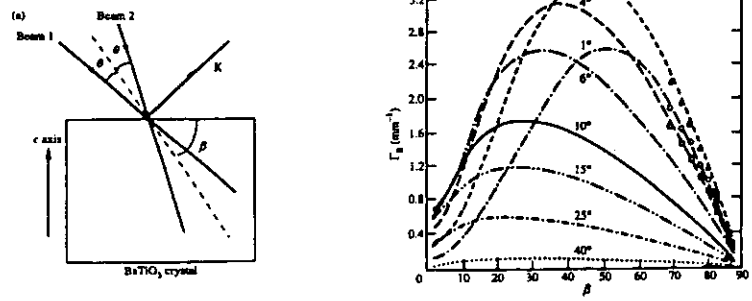

Fainman *et al.*, Opt. Eng. **25**, 228 (1986)

Space-Charge Field and Gain Enhancement

Two Enhancement Techniques
(1) Externally applied DC field with moving fringes
(2) Externally applied AC field

(1)

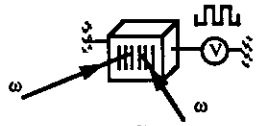

(2)

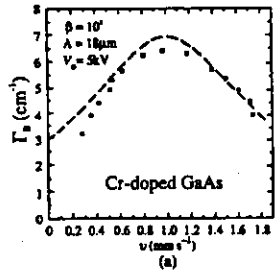

(a)

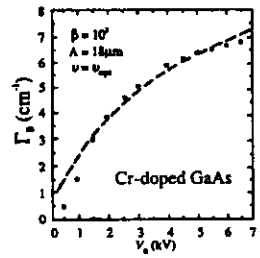

(b)

B. Imbert et al., Opt. Lett. 13, 327 (1988)

Beam Fanning Effect
and
Photorefractive Ring Oscillators

Beam Fanning Effect

If Γ L is too high (e.g., Γ L =20),
then noise signals can be amplified by exp(20) ≈ 5×10^8 !

Unidirectional Ring Oscillator with Photorefractive Gain

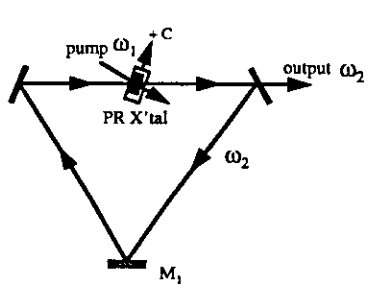

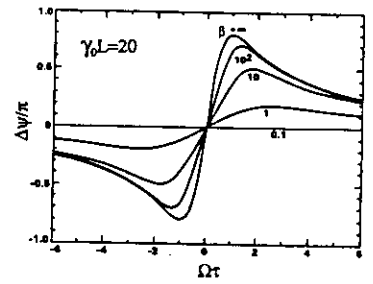

P.Yeh, JOSA B2, 727(1985)

Oscillation Conditions

phase: $\Delta\psi = 2N\pi$+(cavity detuning phase)

amplitude: $2\gamma_0 L > \alpha L - \ln R + 4(\Delta\psi)^2(\alpha L - \ln R)^{-1}$

where

$\gamma = \gamma_0 [1+(\Omega\tau)^2]^{-1}$

$\gamma_0 = 2\pi n_1/\lambda\cos\theta$

$\Omega = \omega_2 - \omega_1$

$= 2\Delta\psi[\tau(\alpha L - \ln R)]^{-1}$

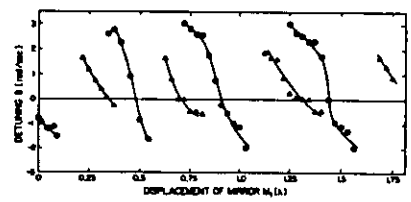

S.K.Kwong *et al.*, JQE QE-22, 1508(1986)

Application to one-way real-time wavefront converters

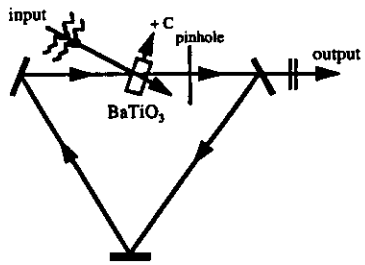

undistorted laser beam

distorted laser beam
after passing through
etched glass plates

corrected output beam

S.K.Kwong *et al.*, JQE QE-22, 1508(1986)

Optical Phase Conjugation and Photorefractive Four-Wave Mixing

Optical Phase Conjugation

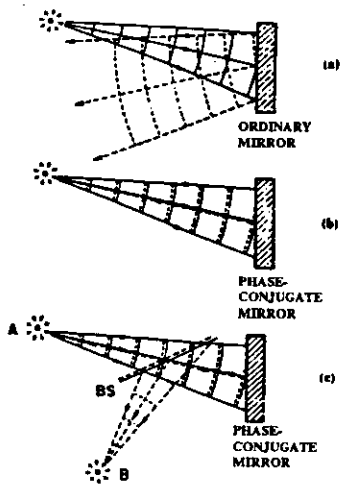

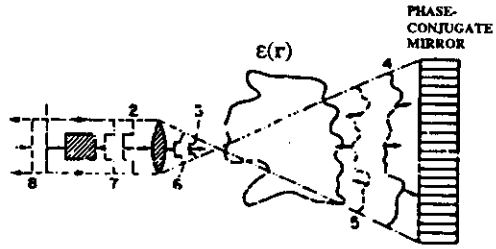

Phase-Conjugate Waves

Input monochromatic wave

$$E_{in}(\mathbf{r},t) = \mathrm{Re}\{A(\mathbf{r})\exp[i(\omega t - kz)]\}$$
$$= \mathrm{Re}\{|A(\mathbf{r})|\exp[-i\phi(\mathbf{r})]\exp[i(\omega t - kz)]\}$$

Phase – conjugate wave

$$E_{pc}(\mathbf{r},t) = \mathrm{Re}\left\{[A(\mathbf{r})\exp(-ikz)]^{*}\exp(i\omega t)\right\}$$
$$= \mathrm{Re}\left\{A^{*}(\mathbf{r})\exp[i(\omega t + kz)]\right\}$$
$$= \mathrm{Re}\{|A(\mathbf{r})|\exp[i(\omega t + kz + \phi(\mathbf{r}))]\}$$
$$= \mathrm{Re}\{|A(\mathbf{r})|\exp[i(-\omega t - kz - \phi(\mathbf{r}))]\}$$
$$= \mathrm{Re}\{[A(\mathbf{r})\exp(-ikz)]\exp[i\omega(-t)]\}$$

Time-reversed wave !

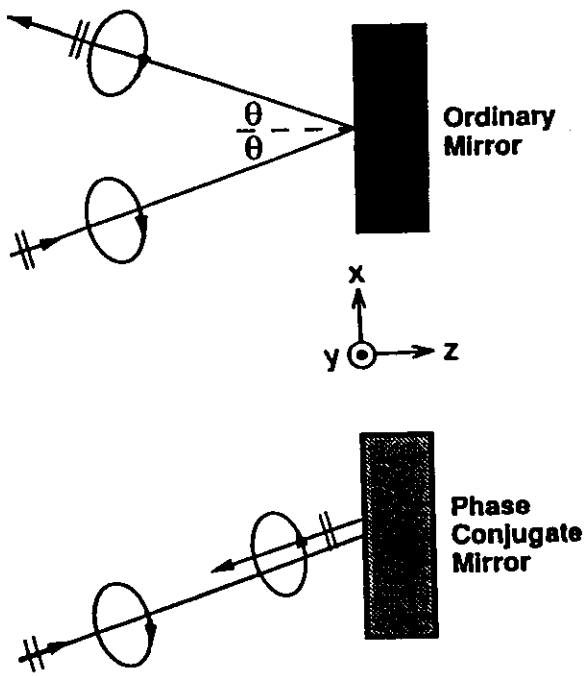

INTERFERENCE FRINGE PATTERNS

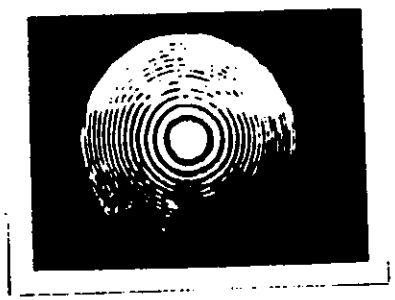

(a) without a glass plate

(b) with a glass plate inserted at A

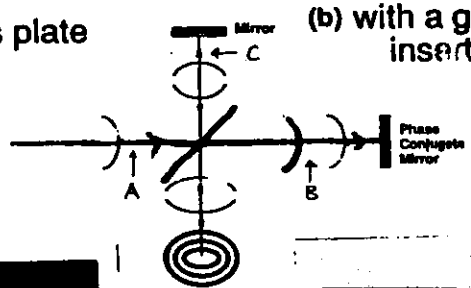

(c) with a glass plate inserted at B

(d) with a glass plate inserted at C

Optical Phase Conjugation by Four-Wave Mixing

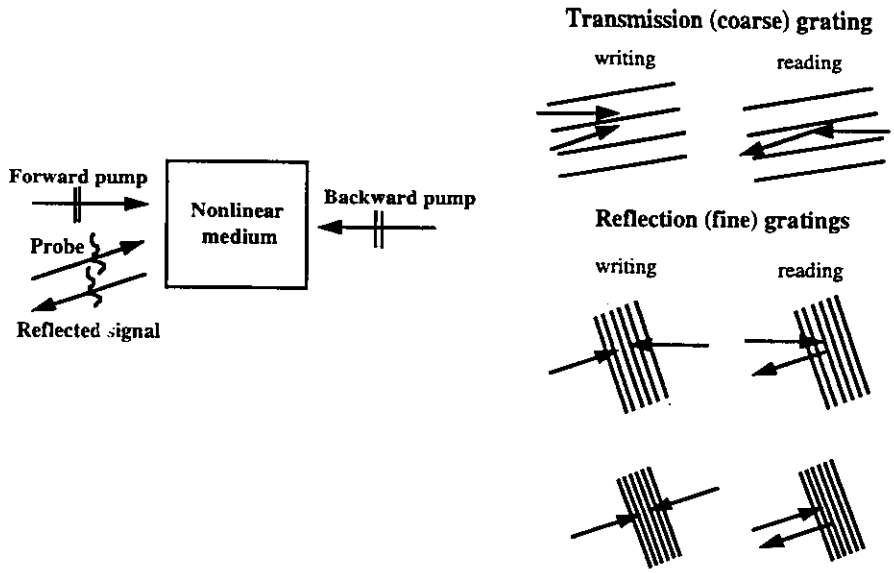

Four-Wave Mixing in a Photorefractive Medium

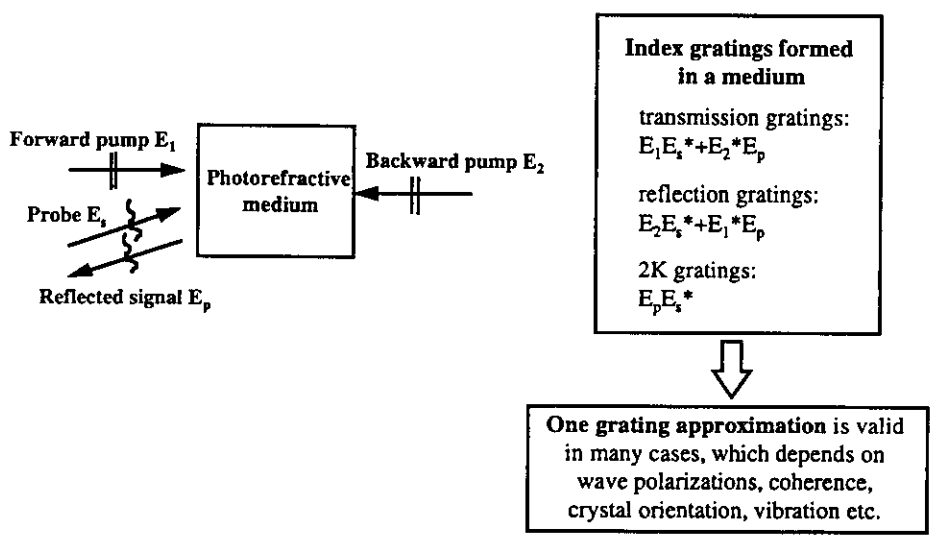

Four-Wave Mixing with Transmission Gratings

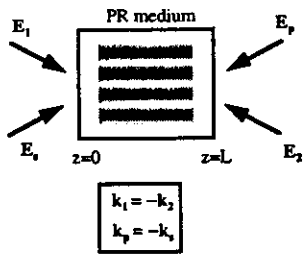

$$\frac{dE_s}{dz} = -\gamma\left(E_s E_1^* + E_2 E_p^*\right)E_1 / I_0$$

$$\frac{dE_1}{dz} = \gamma^*\left(E_s^* E_1 + E_2^* E_p\right)E_s / I_0$$

$$\frac{dE_2}{dz} = \gamma\left(E_s E_1^* + E_2 E_p^*\right)E_p / I_0$$

$$\frac{dE_p}{dz} = -\gamma^*\left(E_s^* E_1 + E_2^* E_p\right)E_2 / I_0$$

where

$$I_0 = I_s + I_1 + I_2 + I_p$$

Constants of integration:

$$\left.\begin{aligned} |E_s|^2 + |E_1|^2 &= c_1 \\ |E_2|^2 + |E_p|^2 &= c_2 \end{aligned}\right\} \text{ conservation of energy}$$

$$E_s E_p + E_1 E_2 = c_3 \quad \text{reciprocity}$$

Four-Wave Mixing with Transmission Gratings

Undepleted pump approximation: $|E_1|^2, |E_2|^2 >> |E_s|^2, |E_p|^2 \Rightarrow dE_1/dz = dE_2/dz \approx 0$

$$\frac{dE_s}{dz} = -\gamma\frac{|E_1|^2}{I_o}E_s - \gamma\frac{E_1 E_2}{I_o}E_p^*$$

$$\frac{dE_p^*}{dz} = -\gamma\frac{|E_2|^2}{I_o}E_p^* - \gamma\frac{E_1^* E_2^*}{I_o}E_s$$

Phase – conjugate reflection coefficient

$$\rho \equiv \frac{E_p(0)}{E_s^*(0)} = \frac{1-\exp(-\gamma^* L)}{1+q\exp(-\gamma^* L)}\left(\frac{E_2}{E_1^*}\right)$$

With $E_p(L) = 0$ and a given $E_s(0)$

$$E_s(z) = \frac{\exp(-\gamma z) + q\exp(-\gamma L)}{1+q\exp(-\gamma L)}E_s(0)$$

$$E_p^*(z) = \frac{\exp(-\gamma z) - \exp(-\gamma L)}{1+q\exp(-\gamma L)}\left(\frac{E_2^*}{E_1}\right)E_s(0) \Rightarrow \quad E_p(0) \propto E_s^*(0)$$

where $q \equiv |E_2|^2 / |E_1|^2$

Phase-Conjugate Reflectivity

PC reflectivity under one transmission grating/undepleted pump approximations

$$R = \left| \frac{\sinh(\gamma L/2)}{\cosh(\gamma L/2 - \ln\sqrt{q})} \right|^2$$

where

$\gamma = \gamma' + i\gamma''$

q = pump int ensity ratio

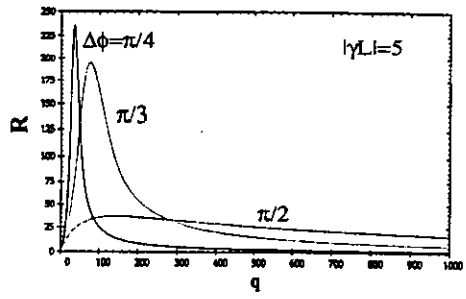

Yeh, Introduction to NLO(1993)

i) diffusion operation($\phi = \pi/2$)

$R_{max} = \sinh^2(\Gamma L/4)$ when $q_{opt} = \exp(\Gamma L/2)$

$\Rightarrow R_{max} \geq 100\%$ for $\Gamma L \geq 4\ln(1+\sqrt{2}) \approx 3.52$ **GAIN!**

ii) drift operation($\phi \neq \pi/2$)

$$R_{max} = \left| \frac{\sinh(\gamma L/2)}{\cos(\gamma'' L/2)} \right|^2 \quad \text{when } q_{opt} = \exp(\Gamma L/2)$$

$\Rightarrow R_{max} \to \infty$ for $\gamma'' L = (2N-1)\pi$ **SELF OSCILLATION!**

Self-Pumped Phase-Conjugate Mirrors (SPPCM's)

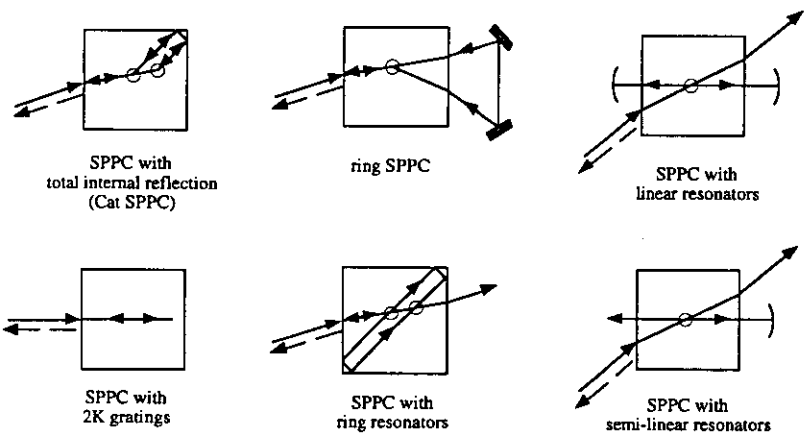

SPPCM's

(a) Linear SPPC: $\gamma_{th}L = 0$

- self-starting
- critical to misalignment
- long coherence length

(b) Semi-linear SPPC: $\gamma_{th}L = 2.49$

- can be self-starting
- critical to misalignment
- long coherence length

(c) Ring SPPC: $\gamma_{th}L = 1.0$

- can be self-starting easily
- robust against misalignment
- no coherence length requirement

(d) Cat SPPC: $\gamma_{th}L = 4.68$

- can be self-starting
- robust against vibration
- short coherence length
- compact

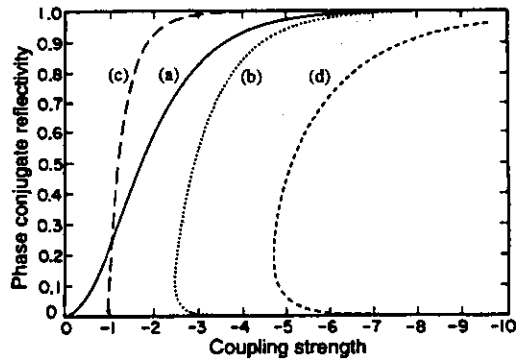

Cronin-Golomb et al., JQE 20, 12(1984)

SELF-PUMPED PHASE-CONJUGATE MIRROR USING INTERNAL REFLECTION

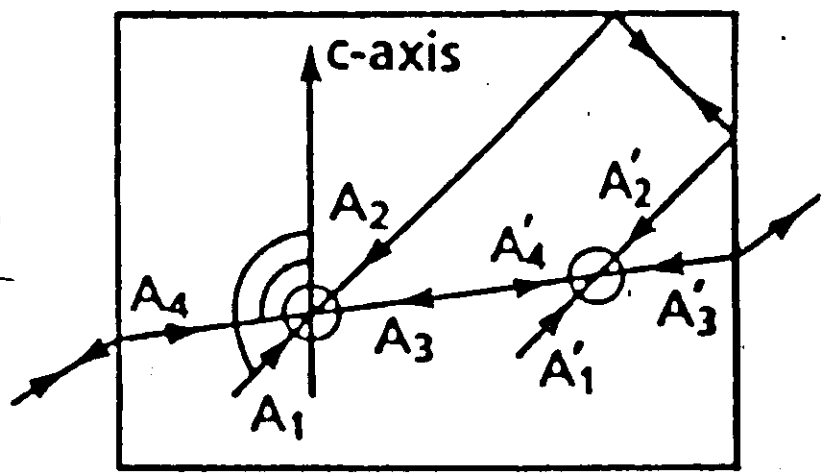

$P3 \propto A1A2A4^*$

22

DYNAMICS OF SELF-ORGANIZING PHASE CONJUGATION

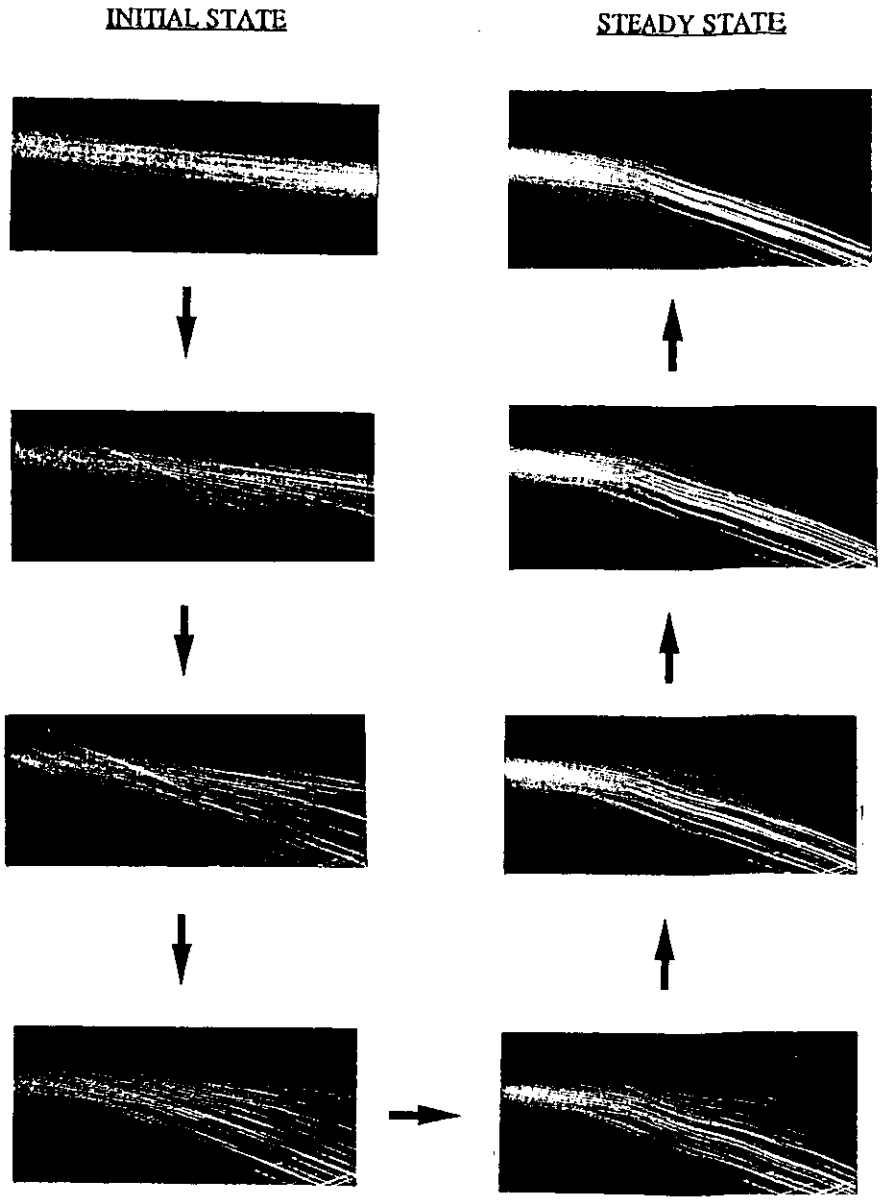

A.Zozulya *et al.* (1994)

Phase shift of SPPCM

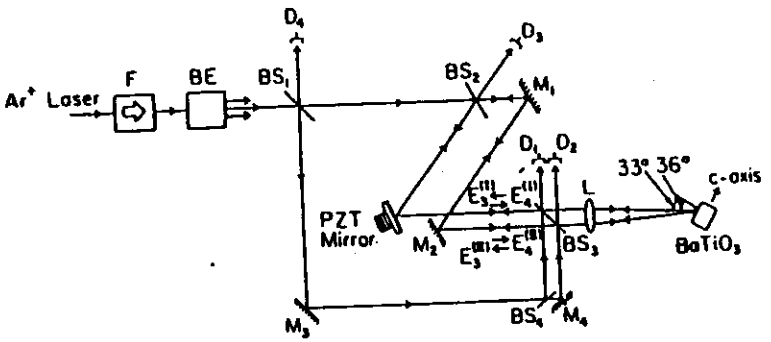

(Y. Tomita et al., 1989)
Opl. Commun. 93, 118-118

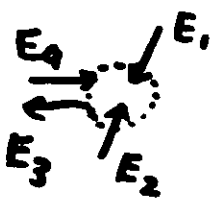

$$E_3 \propto E_1 E_2 E_4^*$$

$$\phi_3 \propto \phi_1 + \phi_2 - \phi_4$$

$$\boxed{\phi_3 \to \phi_3 + \delta \text{ as } \phi_4 \to \phi_4 + \delta}$$

SINCE

$$\phi_{1,2} \to \phi_{1,2} + \delta$$

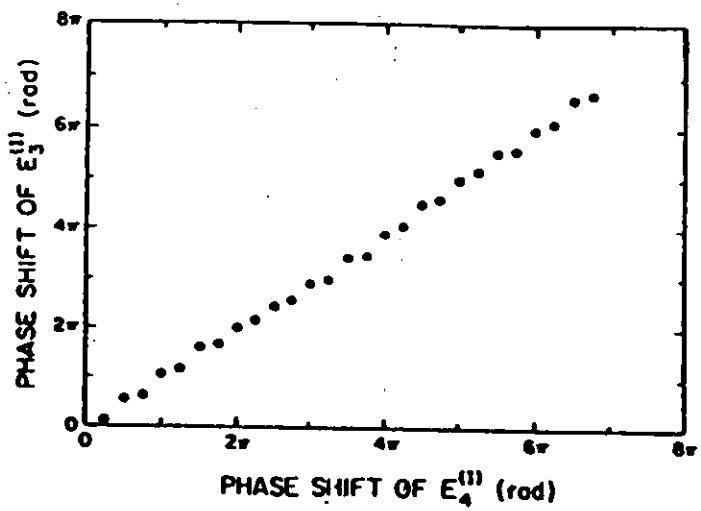

(a)

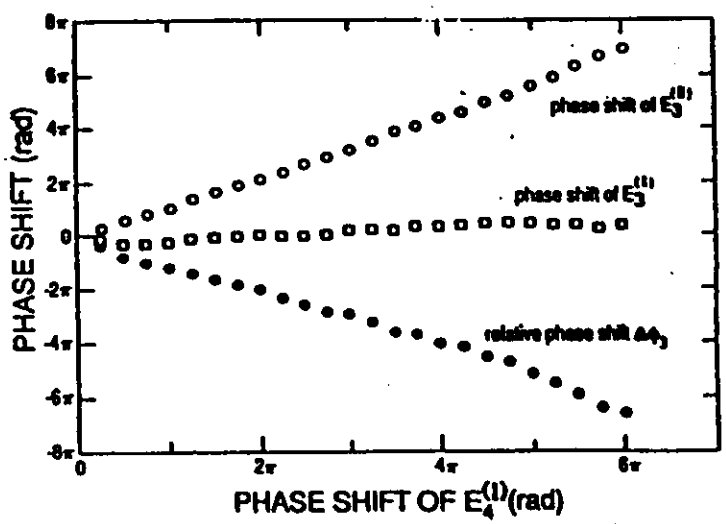

(b)

Mutually Pumped Phase-Conjugate Mirrors (MPPCM's)

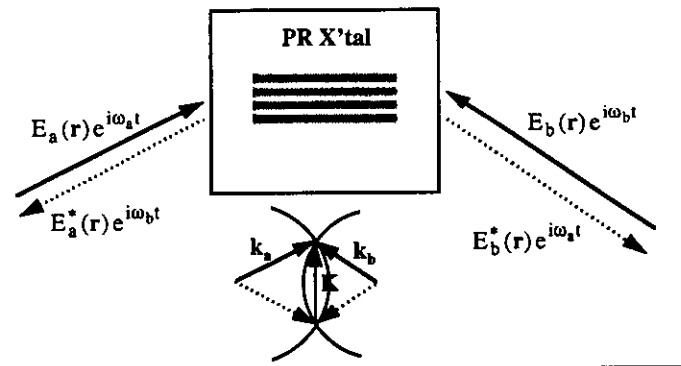

- One phase-conjugate beam originates from the other input
- Two beams prefer to be mutually incoherent
- Wavefronts of input beams prefer to be spatially distorted

Several Configurations for MPPCM's

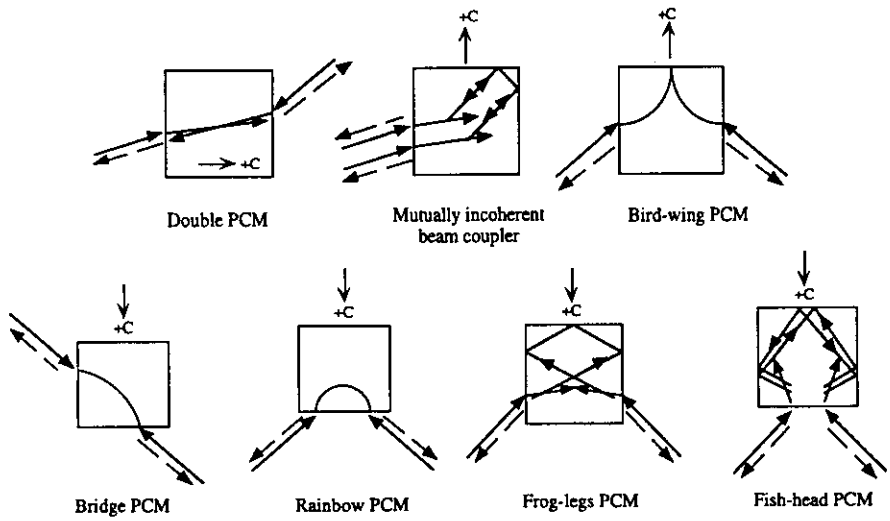

Proposed Models for MPPCM's

- Self-Oscillation Model
  - 1 interaction region (Cronin-Colomb *et al.*, 1984)
  - 2 interaction regions (He, 1988)
- Resonator Model (Yeh *et al.*, 1988)
- Hologram Sharing Model (Ewbank, 1988)

Photorefractive Materials
– figures of merit –

Steady-State Performance

i) Maximum change in the refractive index

$$\Delta n_{max} = \frac{1}{2} n_b^3 r_{eff} E_{sc} \propto \begin{cases} n_b^3 r_{eff} & \text{(diffusion limit)} \\ \dfrac{n_b^3 r_{eff}}{\varepsilon_r} & \text{(trap limit)} \end{cases}$$

ii) Response time of the space-charge field

$$\tau = \frac{\text{write or erase energy}}{\text{average intensity}} = \tau_{di}\left(1 + \frac{4\pi^2 L_{diff}^2}{\Lambda^2}\right)$$

$$\approx \begin{cases} \dfrac{h\nu\varepsilon}{\alpha q \mu \tau_R I_0} & \text{for } L_{diff} << \Lambda \text{ (ferroelectrics)} \\ \dfrac{4\pi^2 h\nu\varepsilon k_B T}{\alpha q^2 \Lambda^2 I_0} & \text{for } L_{diff} >> \Lambda \text{ (bulk semiconductors)} \end{cases}$$

where

τ_{di} = dielectric relaxation time

L_{diff} = diffusion length

I_0 = average intensity

α = absorption coefficient

Transient-State Performance

Photorefractive sensitivity

– the index change per absorbed energy per unit volume

$$S = \frac{\Delta n}{\alpha I_0 \tau}$$

$$\rightarrow \begin{cases} \pi \mu \tau_R \left(\dfrac{n_b^3 r_{eff}}{\varepsilon}\right)\left(\dfrac{k_B T}{\Lambda h\nu}\right) & \text{(diffusion limit and } L_{diff} << \Lambda) \\ \dfrac{q}{4\pi}\left(\dfrac{n_b^3 r_{eff}}{\varepsilon}\right)\left(\dfrac{\Lambda}{h\nu}\right) & \text{(diffusion limit and } L_{diff} >> \Lambda) \end{cases}$$

Figures of Merits for Photorefractive Materials

Materials	wavelength	$\varepsilon/\varepsilon_0$	σ_{dark} $(\Omega \cdot cm)^{-1}$	$n^3 r_{eff}$ (pm/V)	$n^3 r_{eff}/\varepsilon$ $(pm/V\varepsilon_0)$	τ at 1W/cm^2 (sec)	S (cm^3/J)
(ferroelectrics)							
$LiNbO_3$	visible	32(ε_{33})	10^{-8}-10^{-19}	330	10.3	>1	10^{-5}
$BaTiO_3$	visible	135(ε_{33})	10^{-12}	1350	10	1	10^{-4}
SBN:60	visible	880(ε_{33})	10^{-11}	2973	3.4	10	10^{-3}
(paraelectrics)							
BSO	visible	56	10^{-15}	82	1.5	10^{-3}	10^{-3}
(semiconductors)							
GaAs	near IR	12.3	10^{-8}	56	4.6	10^{-4}	10^{-2}
ZnTe:V	visible	10.1	10^{-9}	133	13	10^{-4}	10^{-2}
Cr doped AlGaAs /GaAs MQW	near IR	-	10^{-9}	-	-	10^{-5}	10^{2}
(polymers)							
PVK:TNF: DMNPAA	visible	-	-	-	-	10^{-1}	10^{-3}

Photorefractive Materials – inorganic materials –

Ferroelectric Oxides

Typical materials exhibiting large photorefractivities
- **Ilmenite structures ($LiNbO_3$, $LiTaO_3$)**
- **Perovskite structures [$BaTiO_3$, $KNbO_3$, $KTa_{1-x}Nb_xO_3$ (KTN)]**
- **Tungsten-Bronze structures [$Sr_xBa_{1-x}Nb_2O_6$ (SBN), $(Ba_{1-x}Sr_x)_{2-A}(K_{1-y}Na_y)_{2A-2}Nb_2O_6$ (KNSBN)]**

Several properties in common
- **broadband photorefractive sensitivities (visible to near-infrared)**
- **large dielectric and electrooptic constants which are strongly temperature-dependent**
- **hard and nonhygroscopic materials (high-quality surfaces obtainable)**

Lithium Niobate ($LiNbO_3$)

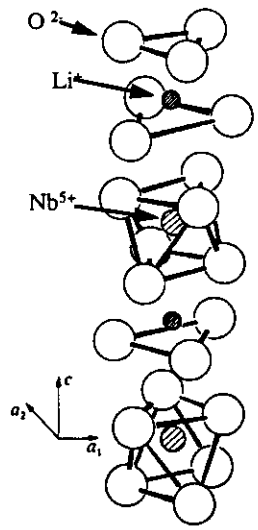

Structual phase transition

Trigonal *3m* (ferroelectric) from R.T. to 1210 ° C

Impurity/defect levels

(deep levels)
Fe^{2+}/Fe^{3+}
Cu^{+}/Cu^{2+}
(shallow level)
intrinsic defect Nb_{Li} (small polaron, Nb^{4+} on Li^{+} site)

Photorefractive effect

(main transport mechamism)
bulk photovoltaic effect / one-center model valid
(dominant charge carriers)
electrons (holes when oxidized)

Nonvolatile Holographic Storage with Two-Color Hologram Recording in $LiNbO_3$

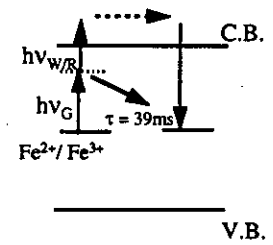

(Sensitization)

$$Nb_{Li}^{5+} + e^- \text{ at } Fe^{2+} \xrightarrow{h\nu_G} Nb_{Li}^{4+}$$

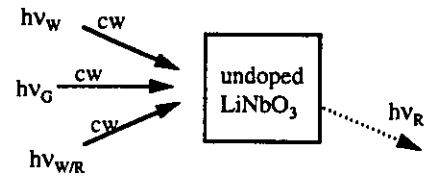

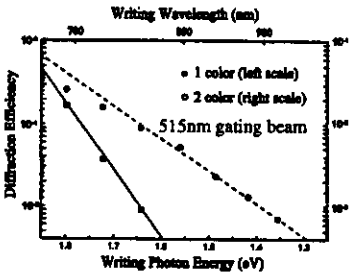

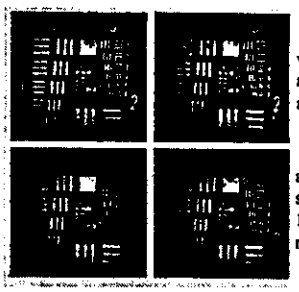

$\lambda_{W/R}$=810nm

virtual image a few min. after writing

after 100 h storage and 10h continuous reading

Bai and Kachru, PRL 78, 2944 (1997)

Barium Titanate ($BaTiO_3$)

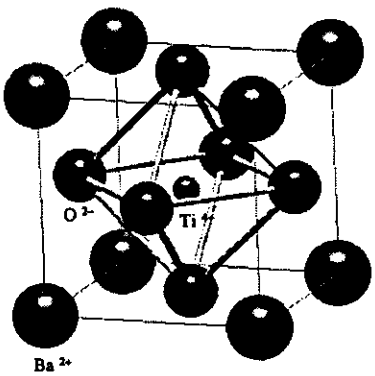

Structual phase transitions

$T \geq 130\,^\circ C$: cubic *m3m* (paraelectric)
$7\,^\circ C \leq T \leq 130\,^\circ C$: tetragonal *4mm* (ferroelectric)
$-90\,^\circ C \leq T \leq 7\,^\circ C$: orthorhombic *mm2* (ferroelectric)

Impurity/defect levels

(deep levels)
Fe^{2+}/Fe^{3+}
Fe^{3+}/Fe^{4+}
Ba^{2+} vacancy
(shallow levels)
O^{2-} vacancy
Ba^{2+} vacancy

The Photorefractive Effect in $BaTiO_3$

Main characteristics

- existence of shallow levels
  - intensity-dependent absorption
  - semi-linear intensity dependence of response time
- increased photorefractivities in visible and near-infrared spectra by doping with cobalt or rhodium

Impurity/defect levels responsible for the PR effect

	PR carriers	major deep levels	shallow levels
As-grown $BaTiO_3$ reduced $BaTiO_3$	holes electrons	Fe^{3+}/Fe^{4+}, Ba^{2+} vacancy	Fe^{4+}/Fe^{5+}, O^{2-} vacancy
Co-doped $BaTiO_3$	holes	Co^{2+}/Co^{3+}, Fe^{3+}/Fe^{4+}	Fe^{4+}/Fe^{5+},
Rh-doped $BaTiO_3$	holes	Rh^{3+}/Rh^{4+}, Fe^{3+}/Fe^{4+}	Rh^{4+}/Rh^{5+}, Fe^{4+}/Fe^{5+}

Photorefractive Properties of Doped $BaTiO_3$

Co-doped $BaTiO_3$

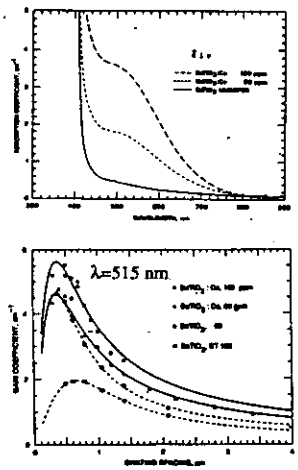

(Rytz *et al.*, 1990)

Rh-doped $BaTiO_3$

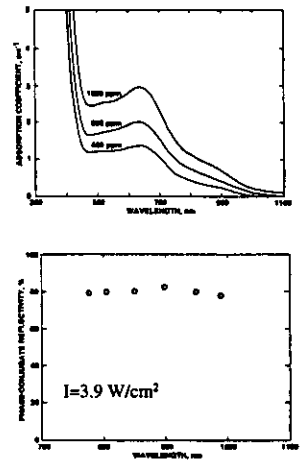

(Wechsler *et al.*, 1994)

Strontium Barium Niobate (SBN)
and
Potassium Sodium Strotium Barium Niobate (KNSBN)

Projection of structure of tetragonal (*4mm*) tungsten bronze parallel to (001)

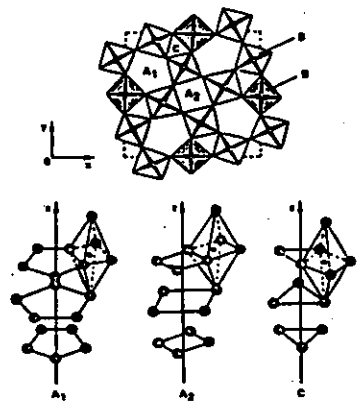

A_1:15-fold;A_2:12-fold;C:9-fold;B:6-fold coordinated sites

Unique Advantages

- extraordinarily large electrooptic coefficients
- structural flexibility due to partially empty sites
- no phase transition at low temperatures
- large size available due to the absence of 90° twins

List of Typical PR Materials belong to $(A_1)_4(A_2)_2B_{10}O_{30}$

composition	r (pm/V)	T_c (°C)	partially empty sites
$Sr_xBa_{1-x}Nb_2O_6$ SBN:60 (x=0.6) SBN:75 (x=0.75)	235(r_{33}) 1340(r_{33})	75 56	15- and 12-fold sites up to 20%
KNSBN	270 (r_{33}) 400 (r_{42})	71	15- and 12-fold sites

Comparison of Photorefractive $BaTiO_3$, SBN and KNSBN

CRYSTAL	SBN, KNSBN	BaTiO3
STRUCTURE	TUNGSTEN-BRONZE	PEROVSKITE
GROWN IN LARGE SIZE	RELATIVELY EASY	DIFFICULT
ε	LARGE ε_{33}(SBN)、ε_{11} (KNSBN)	LARGE ε_{11}、ε_{33}
r	LARGE r_{33}(SBN)、r_{51} (KNSBN)	LARGE r_{51}
COMPOSITIONS CHANGE	EASY	DIFFICULT
DOPING	EASY	DIFFICULT
PHASE TRANSITION POINT BELOW R.T.	NO	NEAR 5°C

ABSORPTION SPECTRA

Cr-doped (0.02 wt.%) SBN:60

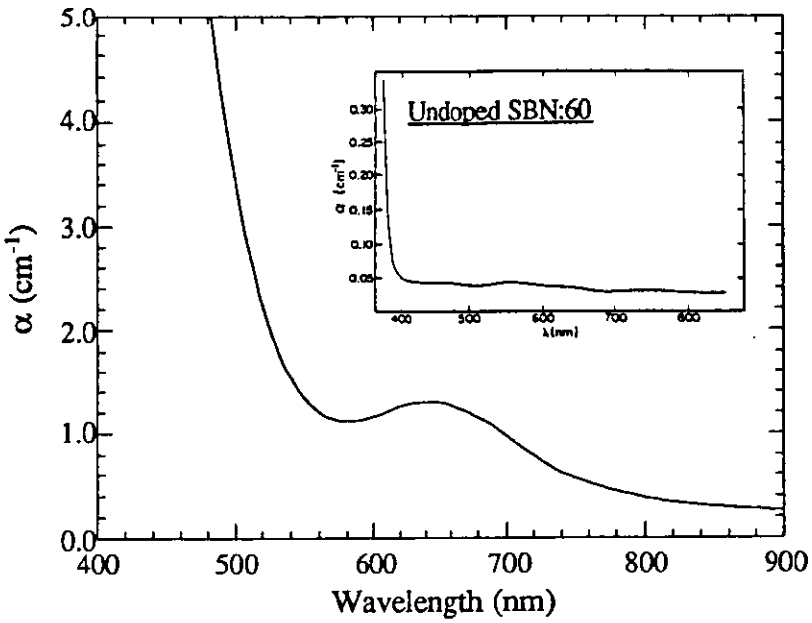

KNSBN

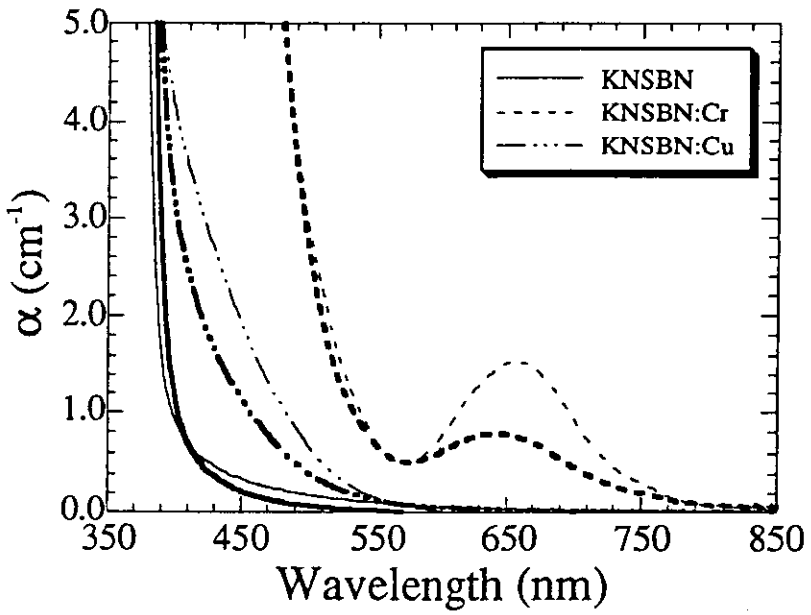

* extraordinary light (bold curves)

Y.Tomita *et al.* (1993)

Grating Spacing Dependence of Γ

Cr-doped SBN:60
(ordinary polarization)

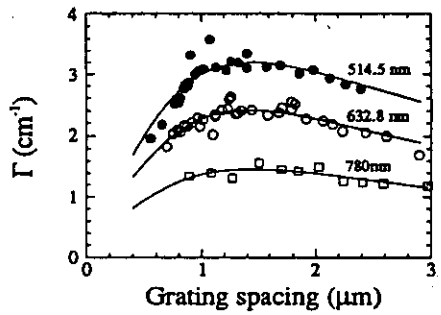

Cr-doped KNSBN
(extraordinary polarization)

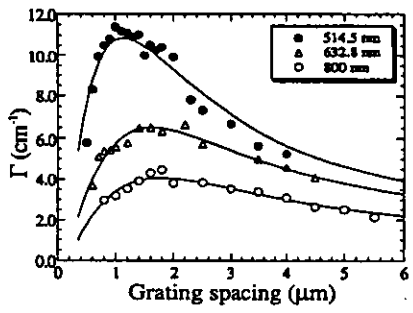

Y.Tomita and A.Suzuki, Opt.Rev.1, 233(1994)

Intensity Dependence of Response Rate

Cr-doped SBN:60
(Λ=1.5 μm)

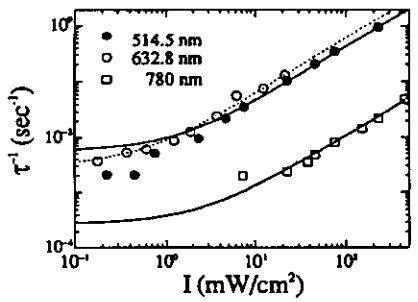

Cr-doped KNSBN
(Λ=1.9 μm)

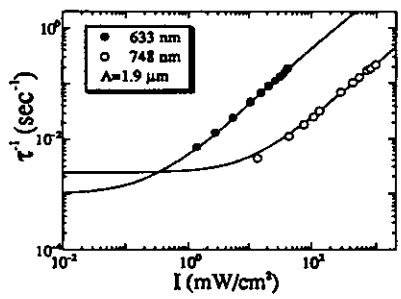

Y.Tomita and A.Suzuki, Opt.Rev.1, 233(1994)

PHOTOREFRACTIVE SPECTRA

MAXIMUM Γ

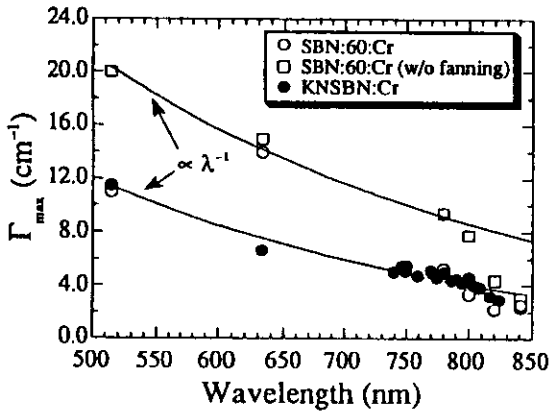

RESPONSE RATE

(I=150mW/cm^2 and Λ=1.5μm)

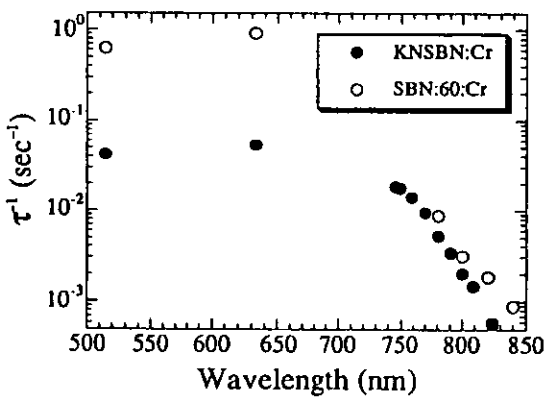

COMPARISON WITH OTHER DOPED CRYSTALS (@λ=840nm)

GAIN COEFFICIENT

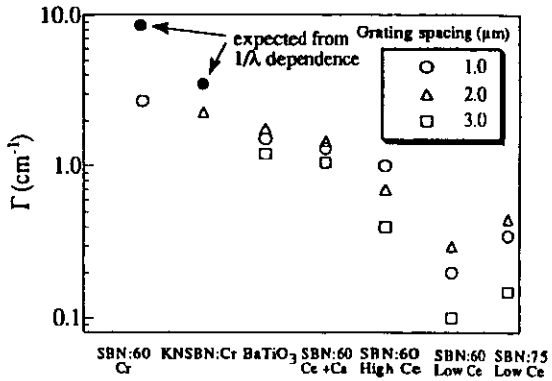

RESPONSE TIME

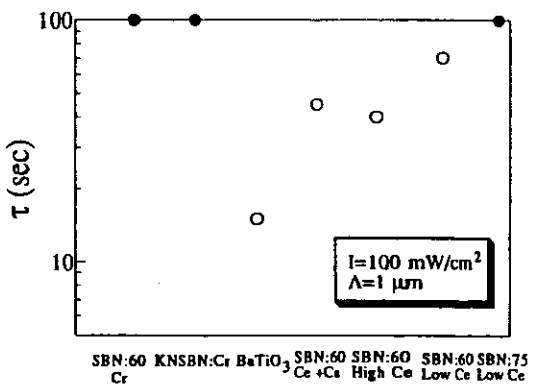

* other data are taken from G.A.Rakuljic, Ph.D. thesis, (Caltech,1987)

Y.Tomita and A.Suzuki (1994)

RELATIONSHIP BETWEEN r AND ε

$$r = 2g\varepsilon_0\varepsilon_s P_s$$

WHERE g : 2ND-ORDER EO COEFFICIENT
P_s : SPONTANEOUS POLARIZATION

$$\begin{pmatrix} r_{13} = 2g_{13}\varepsilon_0\varepsilon_{33}P_s \\ r_{33} = 2g_{33}\varepsilon_0\varepsilon_{33}P_s \\ r_{42} = 2g_{44}\varepsilon_0\varepsilon_{11}P_s \end{pmatrix}$$

POWER-LAW DEPENDENCE

$$\varepsilon_s \propto (T_c - T)^{-\gamma}$$

$$\rightarrow r \propto (T_c - T)^{\delta-\gamma}$$

$\varepsilon_{//}$

$$P_s \propto (T_c - T)^{\delta}$$

SCALING LAW OF Γ

$$\Gamma = \frac{Q_1}{\Lambda}\frac{T(T_c - T)^{\delta}}{(T_c - T)^{\gamma} + Q_2 T/\Lambda^2}$$

SO

$$\Gamma|_{max} \propto (T_c - T)^{\delta-0.5\gamma}\sqrt{T}$$

$$\Lambda_{opt} \propto (T_c - T)^{-0.5\gamma}\sqrt{T}$$

SCALING LAW OF τ^{-1}

$$\tau^{-1} \propto (T_c - T)^{\gamma} + Q_2 T/\Lambda^2$$

TEMPERATURE DEPENDENCE OF Γ (KNSBN:Cr @ λ=632.8 nm)

$T_C = 84.8^{\circ}$ C, $\delta = 0.67$, $\gamma = 1.256$

$\Gamma_0|_{max} \propto (T_c - T)^{\delta-0.5\gamma}\sqrt{T}$ $\Lambda_{opt} \propto (T_c - T)^{-0.5\gamma}\sqrt{T}$

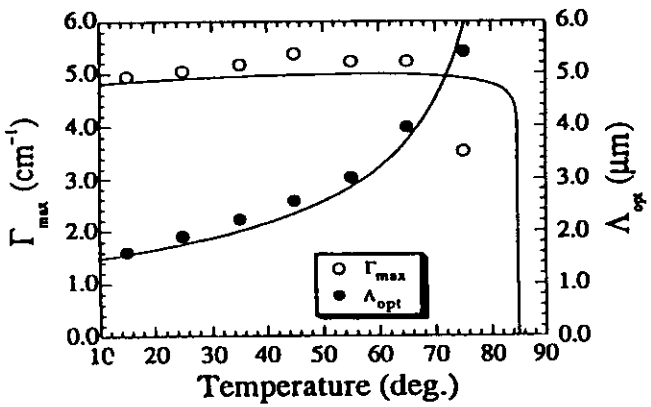

Y. Tomita (1995)

Opt. Materials 4, 281-285 (19

Photorefractive Materials
– semi-insulating semiconductors–

Photorefractive Semiconductors

Typical PR semiconductors/structures
- **Bulk SI semiconductors**
  - **undoped GaAs and GaAs:Cr**
  - **InP:Fe**
  - **CdTe:V**
  - **CdMnTe**
  - **GaP**
- **SI Quantum-well/supperlattice structures**
  - **GaAs/AlGaAs**
  - **ZnTe/CdZnTe**

Major electrooptic phenomena in PR semiconductors/structures
- **Pockels effect**
- **quadratic electrooptic effect via band-edge Franz-Keldysh and quantum-confined Stark/Franz-Keldysh effects**
- **high field effect**
- **picosecond PR effect**

Undoped GaAs

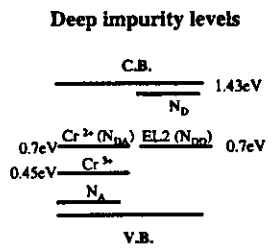

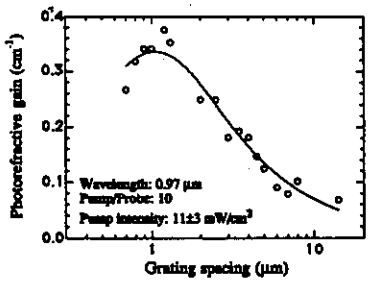

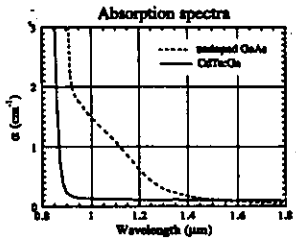

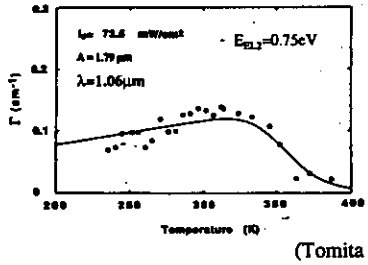

(Tomita *et al.*, 1989)

SPPCM and DPCM Using PR Semiconductors

SPPCM

- InP:Fe at 1.32 μm (Bylsma *et al.*, 1989)

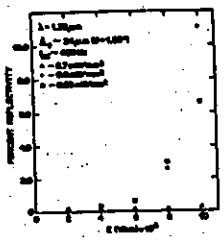

- Undoped GaAs at 1.06 μm (Chua *et al.*, 1990)

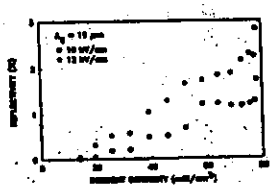

DPCM

- Undoped GaAs at 1.06 μm (Chua *et al.*, 1990)

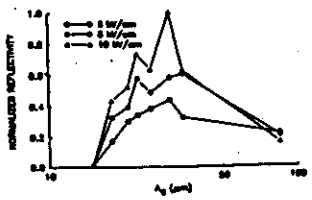

Band-Edge Photorefractive Effect

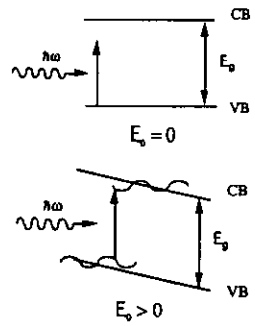

$$\alpha \rightarrow \alpha + \Delta\alpha(E_{total}) \Rightarrow n \rightarrow n + \Delta n(E_{total})$$

where

$$\Delta n(E_{total}) = AE_{total}(x) + BE_{total}^2(x)$$

$$E_{total}(x) = E_0 + E_{sc}(x)$$

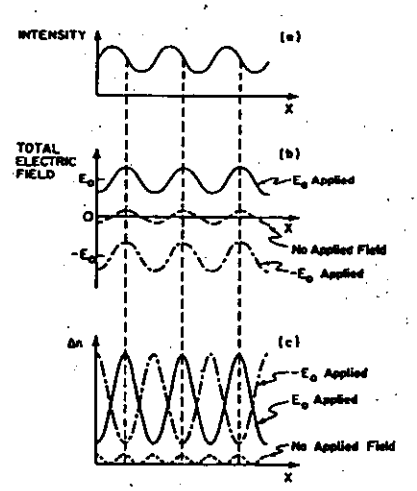

(Partovi et al., 1990)

Band-Edge Photorefractive Effect
– experimental results –

Undoped GaAs

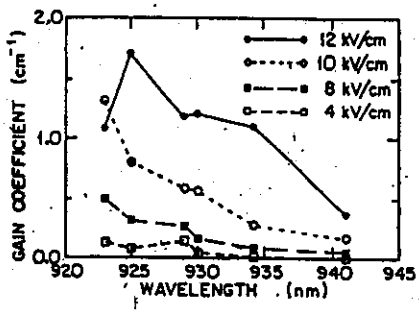

(Partove et al., 1990)

InP:Fe

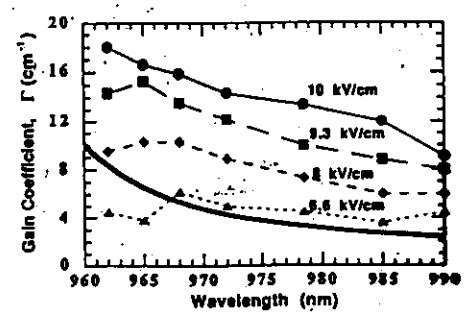

(Millerd et al., 1990)

Resonant Photorefractive Effect in Semi-Insulating Quantum Wells

photorefractive effect
(holographic gratings)
+
quantum-confined Stark/Franz-Keldysh effects
(large nonlinearities and fast response)

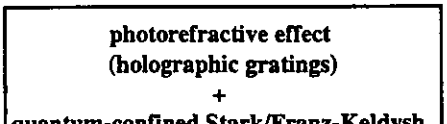

use of semi-insulating quantum wells

$$\Delta n \propto E^2$$

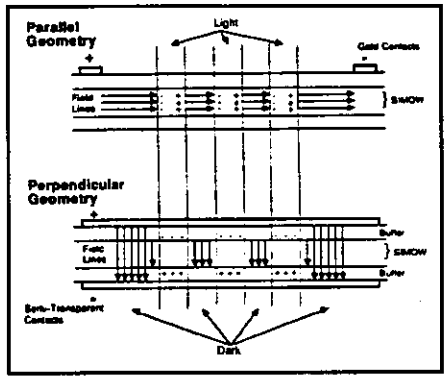

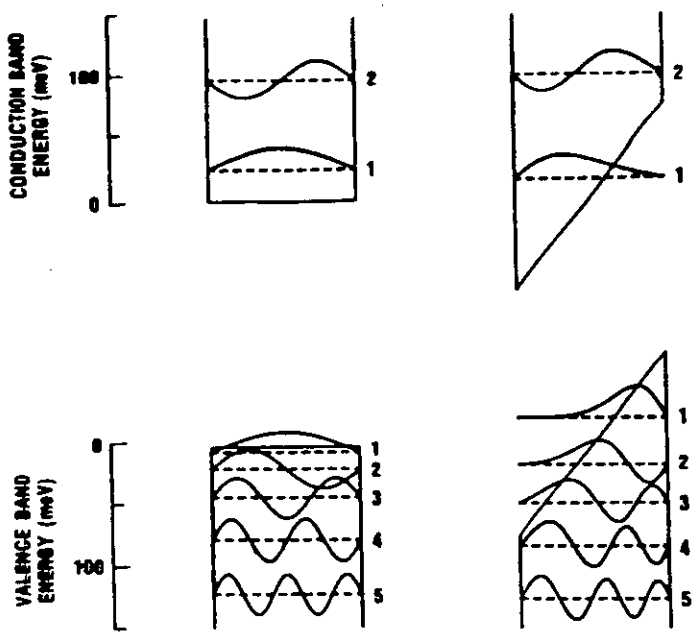
CONDUCTION BAND ENERGY (meV)
100
0
2
1
2
1
VALENCE BAND ENERGY (meV)
0
100
1
2
3
4
5
1
2
3
4
5

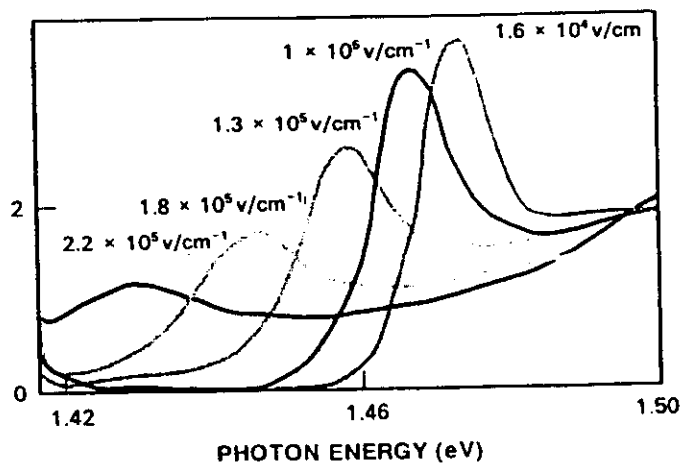
1.6 × 10⁴ v/cm
1 × 10⁶ v/cm⁻¹
1.3 × 10⁵ v/cm⁻¹
1.8 × 10⁵ v/cm⁻¹
2.2 × 10⁵ v/cm⁻¹
2
0
1.42
1.46
1.50
PHOTON ENERGY (eV)

Photorefractive GaAs/AlGaAs Quantum Wells (parallel geometry)

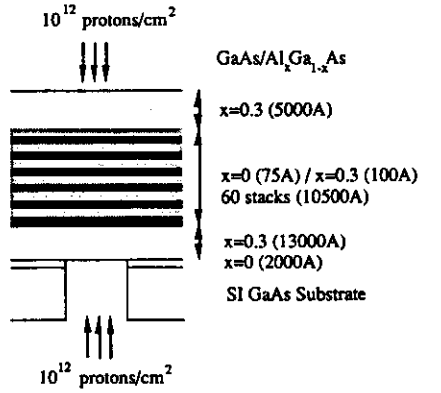

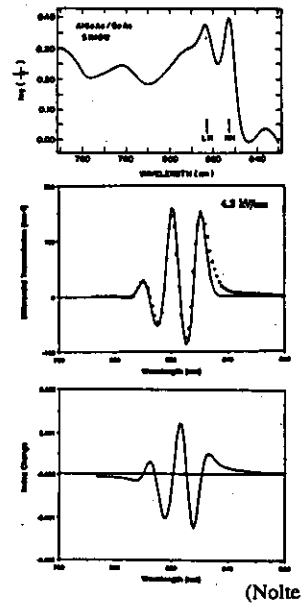

$\sigma_{dark} = 10^{-9}(\Omega \cdot cm)^{-1} << \sigma_{photo}$ for $I \geq 1mW/cm^2$

(Nolte *et al.*, 1990)

Diffraction Efficiencies of photorefractive GaAs/AlGaAs Quantum Wells

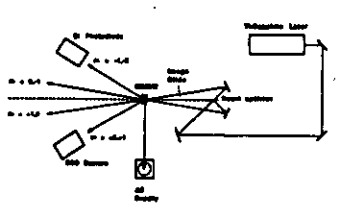

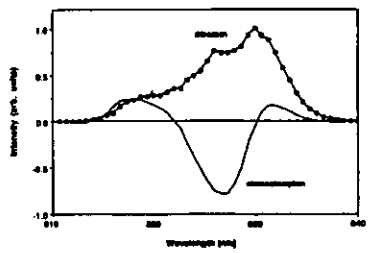

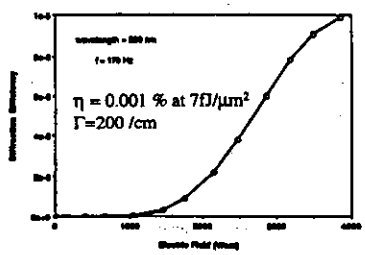

Advantages of Photorefractive GaAs/AlGaAs Quantum Wells

- low saturation intensity I_{sat}

$$I_{sat} = \frac{\hbar\omega\sigma_{dark}}{e\mu\tau_R\alpha} = 100\text{nW/cm}^2 \approx \frac{I_{sat}(\text{bulk})}{10000}$$

- fast response τ

$$\tau = \tau_{di}\left[1+\left(\frac{2\pi\mu\tau_R E}{\Lambda}\right)^2\right] = 100\mu\,\text{sec} = \frac{\tau(\text{bulk})}{10000}$$

for $I = 100\text{mW/cm}^2$ and $E = 10^4\,\text{V/cm}$

- low switching energy E_{sw}

$$E_{sw} = I\tau = 155\text{fJ}/\mu\text{m}^2 \text{ for } E = 10^4\,\text{V/cm}$$

- high PR sensitivity S

$$S = \frac{\Delta n_{resonance}}{\alpha I\tau} \le 10^{-2}\text{cm}^3/\text{J} \approx 10^4\,S(\text{bulk})$$

- large refractive index changes $\Delta n_{resonance}$

$$\Delta n_{resonance} \approx 2\Delta n(\text{bulk})E(\text{cm/V}) = 10^4\,\Delta n(\text{bulk}) \text{ at } E = 5\text{kV/cm}$$

These advantages can be attributed mainly to large quadratic electrooptic effects and large linear absorption.

Picosecond Photorefractive Effect

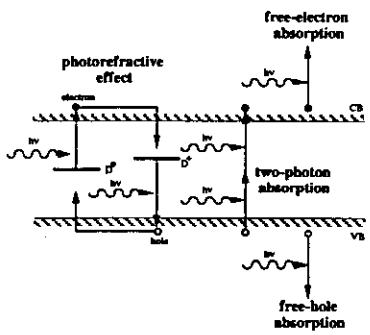

Experimental setup for picosecond beam coupling

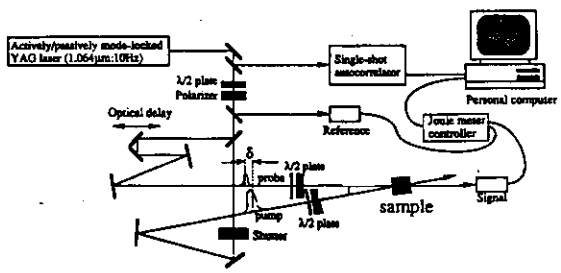

Nonlinear transmit tan ce change

$$\Delta T = \frac{T(\text{w/ pump}) - T(\text{w/o pump})}{T(\text{w/o pump})}$$

Picosecond Photorefractive Effect in Undoped GaAs

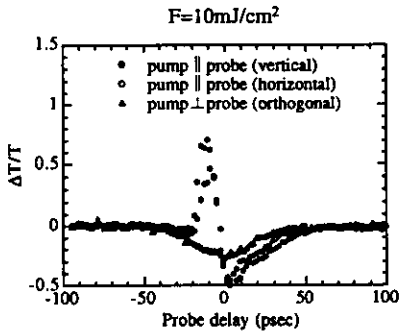

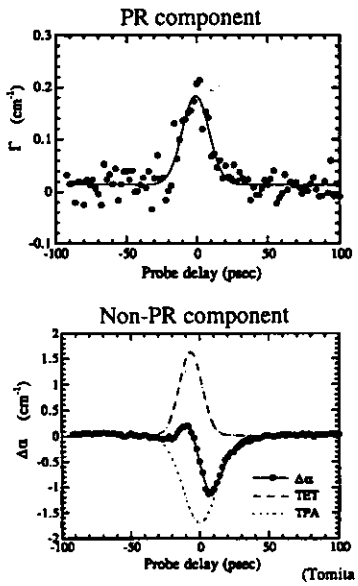

(Tomita *et al.*, 1992)

Picosecond Polarization Switching Using SI CdTe:Ga

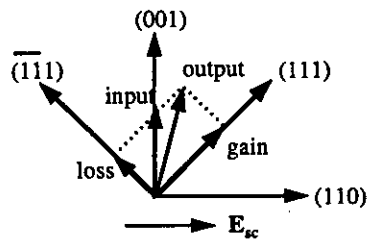

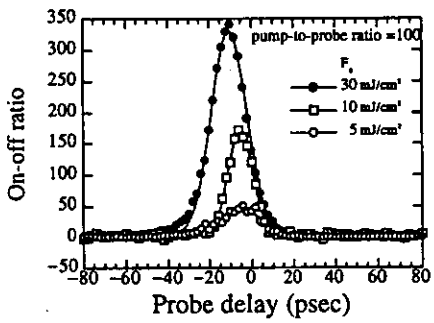

Tomita and Enami., APL 66,.914(1995)

Photorefractive Materials
– organic materials –

Photorefractive Polymers

- First reported by Ducharme et al.*
- Incorporate charge-generation materials, charge-transfer materials, and NLO entities
- Three families of polymeric PR materials

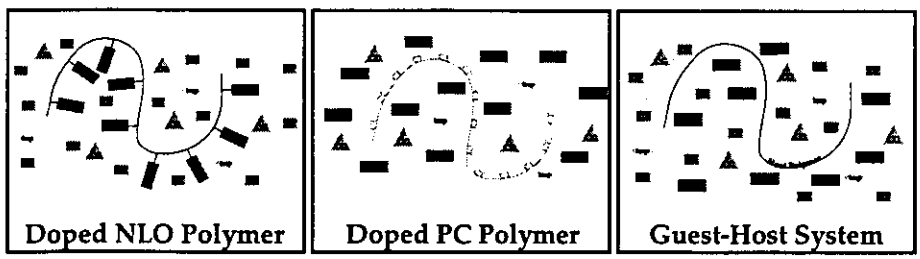

*S. Ducharme, J.C. Scott, R.J. Twieg, and W.E. Moerner, Phys. Rev. Lett. 66, 1846-49 (1991).

Space-Charge Field Formation Process in a Photorefractive Polymer

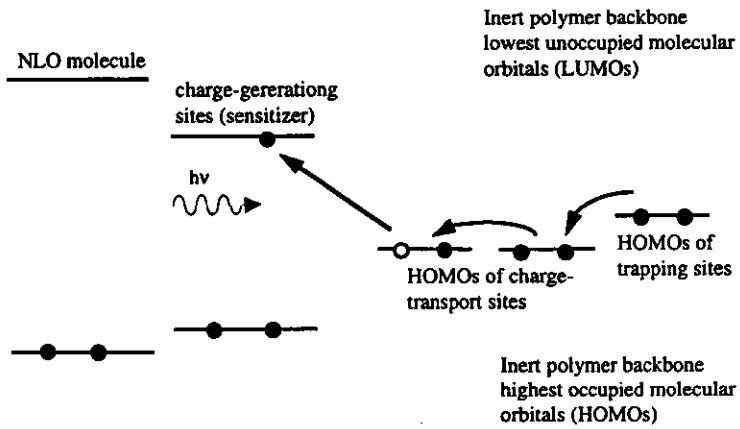

Reported Material Systems for Photorefractive Polymers

Material System	λ (nm)	η_{diff}	Γ_{2BC} (cm^{-1})	Type
bis-A-NPDA:DEH	647	5×10^{-5}	0.33	NLO
PMMA-PNA:DEH:C_{60}	647	4.8×10^{-5}	0.6	NLO
PVK:TNF:EPNA	633	2×10^{-3}	18	PC
PVK:TNF: DMNPAA:ECz	675	8.6×10^{-1}	207	PC
PVK:TNF:DR1:ECz	700	1.6×10^{-5}	---	PC
PBPES:TNF:FDEAMNST	676	1.3×10^{-2}	9.9	PC
PMMA:DEH:NPP:SQ	633	1.1×10^{-2}	10	G-H

*NLO = NLO polymer; PC = photoconducting polymer; G-H = guest-host system

Main Characteristics of Photorefractive Polymers

1. Application of external field:
   a) Poling for NLO
   b) Photoconduction:
      carrier generation
      carrier mobility
      ➡ function of externally applied field (E_0)

2. Orientation enhancement effect†
   - Enhancement of PR effect due to modulated birefringence

†W.E. Moerner, S.M. Silence, F. Hache, and G.C. Bjorklund, J. Opt. Soc. Am. B 11, 320-30 (1994)

Orientation Enhancement Effect in Low-Glass Transition Temperature Photorefractive Polymers

NL chromophores are aligned according to the total poling field given by

$$E_{total}(r) = E_0 + E_{sc}(r)$$
$$= [E_{sc}(r)\sin\theta]e_x + [E_0 + E_{sc}(r)\cos\theta]e_z$$

Orientational birefringence contribution

$$\Delta n^s_{BR} \propto -N\mu^2\Delta\alpha E_0 E_{sc}$$

$$\Delta n^p_{BR} \propto N\mu^2\Delta\alpha E_0 E_{sc}$$

where

$$\Delta\alpha = \alpha_{//} - \alpha_{\perp}$$

Electrooptic conribution

$$\Delta n^s_{EO} \propto N\mu\beta E_0 E_{sc}$$

$$\Delta n^p_{BR} \propto N\mu\beta E_0 E_{sc}$$

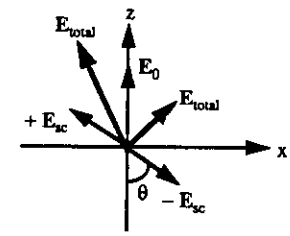

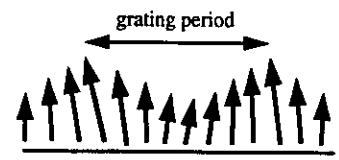

PVK:TNF:DMNPAA:ECz

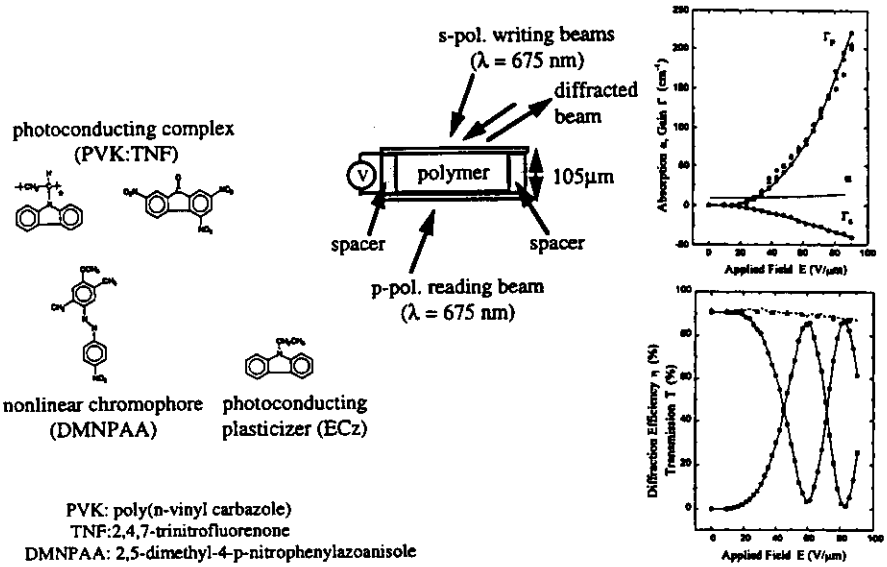

PVK: poly(n-vinyl carbazole)
TNF:2,4,7-trinitrofluorenone
DMNPAA: 2,5-dimethyl-4-p-nitrophenylazoanisole
ECz: n-ethylcarbazole

K.Meerholz et al., Nature **371**, 497(1994)

Self-Pumped Phase Conjugation with Photorefractive Polymer Stacks

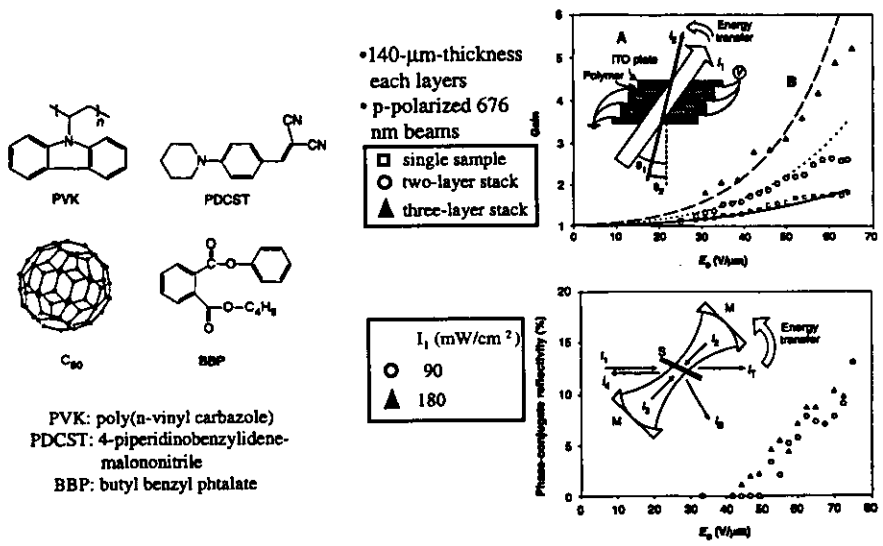

PVK: poly(n-vinyl carbazole)
PDCST: 4-piperidinobenzylidene-malononitrile
BBP: butyl benzyl phtalate

Grunnet-Jepsen *et al.*, Science **277**, 549(1997)

Photorefractive Polymer-Dispersed Liquid Crystals

Main advantages
- **high index changes with much lower electric fields (a few V/cm)**
- **high resolution of photorefractive polymers**

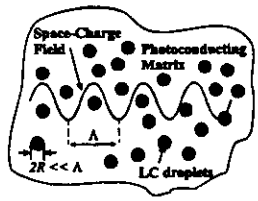

PMMA:E49:TNF:ECz
<2R>= 0.25μm
sample thickness = 53 μm

torque induced by E_0+E_{sc} = elastic torque

➡ $\Delta n \propto E_0 E_{sc}$

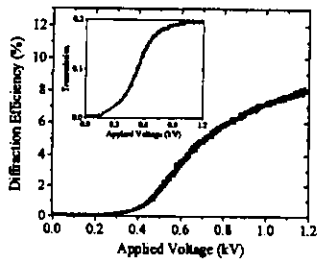

λ_{write} = 633 nm (1mW)
λ_{read} = 675 nm (10μW)

No higher-order diffraction

⬇

Bragg diffraction regime

$\Delta n = 2 \times 10^{-3}$ at 1.2 kV
Γ = 41 /cm (α=735/cm) at 0.3 kV

A. Golemme *et al.*,Opt. Lett. **22**,1226(1997)

Applications

Possible Applications of Photorefractive Nonlinearities

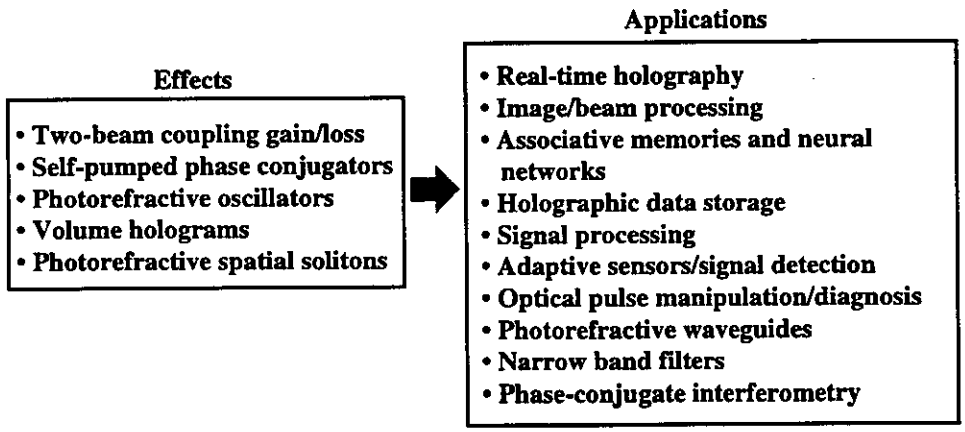

Applications of Two-Beam Coupling to Image/Beam Processing

Use of photorefractive gain
- **Coherent image amplification**
- **Beam cleanup**
- **Laser power combining**
- **Adaptive sensors/signal detection**
- **Pulse shaping**
- **Novelty filters**
- **Optical interconnect**

Use of photorefractive loss
- **Optical limiters**
- **Novelty filters**
- **Pulse shaping**

Laser Beam Cleanup and Amplification

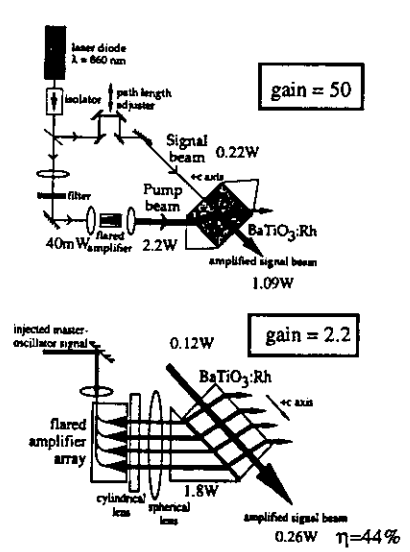

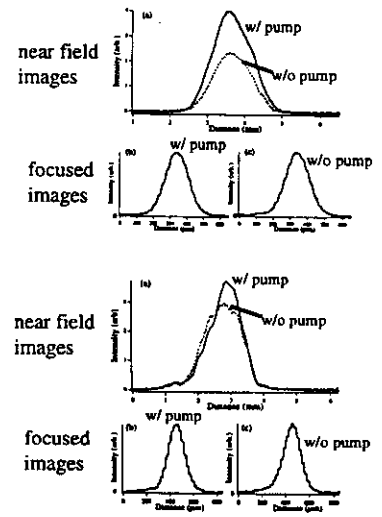

S.MacCormack *et al.*,Opt. Lett.**22**, 227(1997)

Tracking Novelty Filters

Function

- Detection of time-dependent features in a scene
- Temporal differentiation of a moving image

Implementation

Use of Transient Photorefractive Gain

S.K.Kwong *et al.*,
JOSA B 5, 1788 (1988)

amplitude or phase image

Use of Photorefractive Loss

M.Cronin-Golomb *et al.*,
Opt.Lett. 12, 1029 (1987)

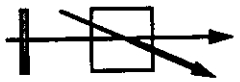

phase image

Use of Phase-Conjugate Waves

D.Z.Anderson *et al.*,
Opt.Lett. 12, 123 (1987)

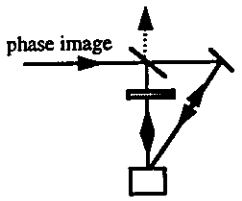

Tracking Novelty Filter Using Trensient Energy Transfer – principle of operation –

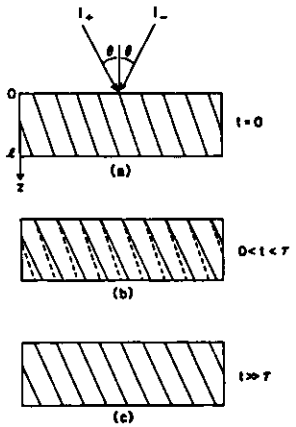

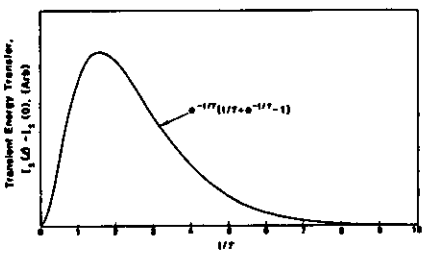

Tracking Novelty Filter Using Trensient Energy Transfer – experimental setup –

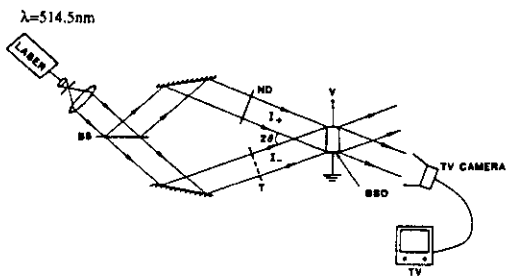

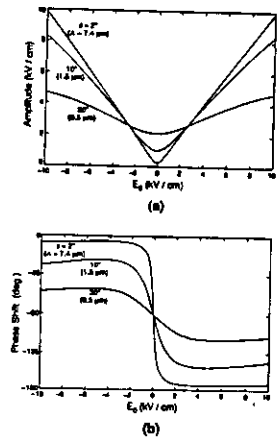

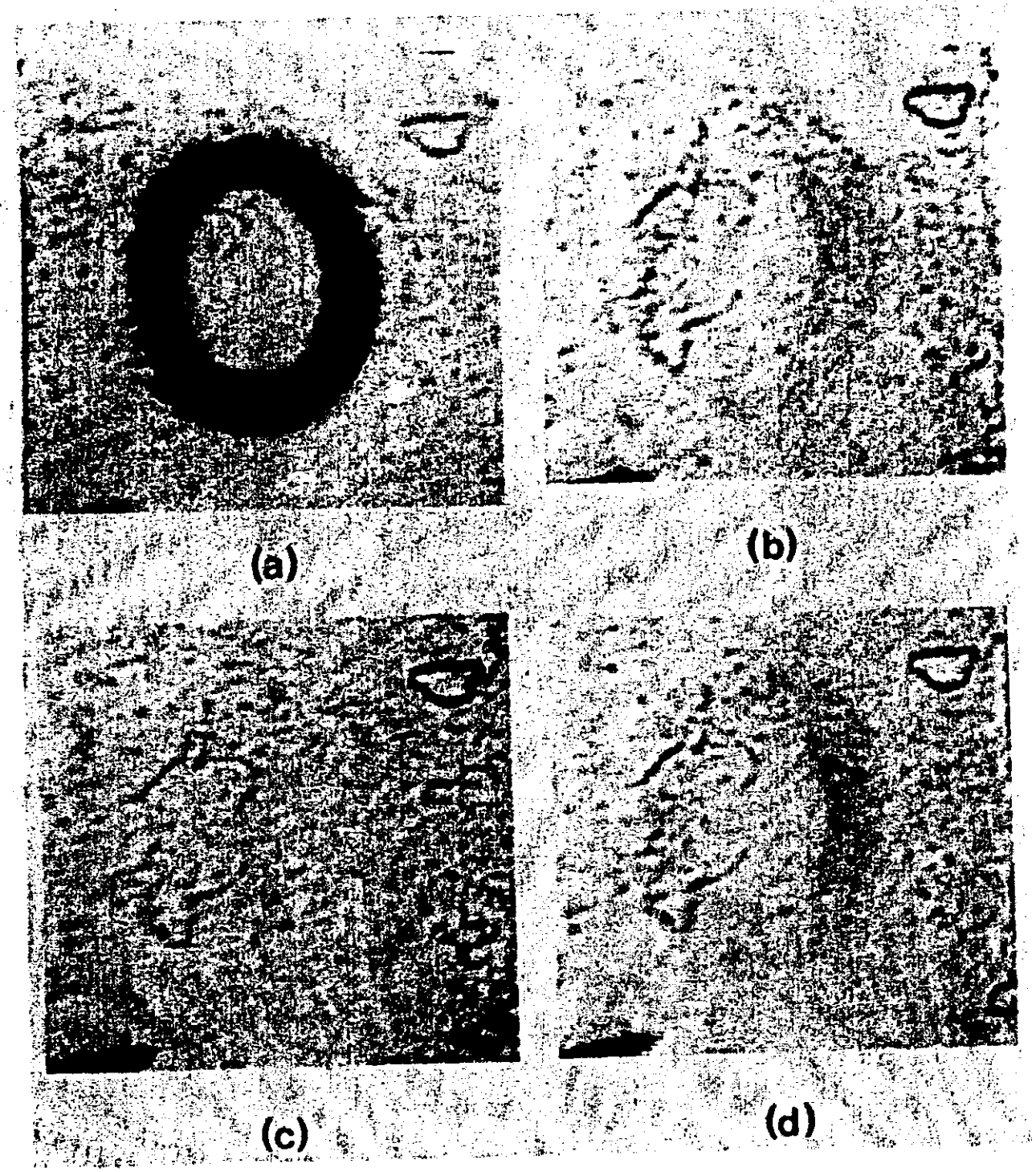
(a)
(b)
(c)
(d)

Applications of Photorefractive Volume Holograms

- Holographic data storage
- Image processing
- Matrix operation
- Spatial light modulation
- Optical pulse manipulations/diagnosis/storage
- Narrow band filters

Real-Time Image Processing

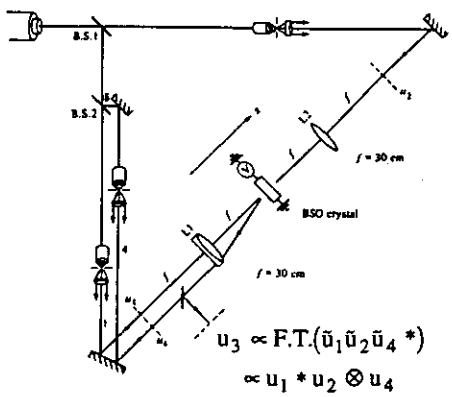

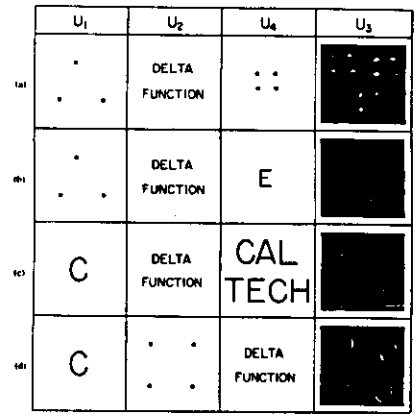

J.O.White *et al.*,APL40,450(1982)

Nonlinear Optical Matrix Processor
– principle of operation –

Recording

• Matrix-matrix multiplications by use of grating degeneracy

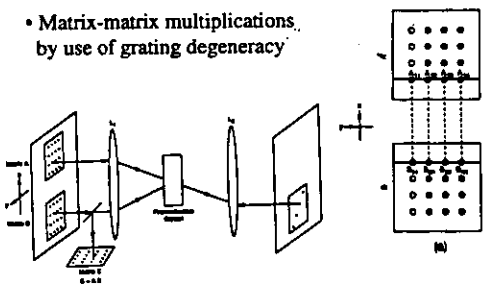

• N^2 gratings formed along the x direction
• N^3 gratings in the volume
• N degenerate gratings for each grating K vector

$$\Delta n \propto \frac{1}{I_0} \mathrm{Re}[(A_{11}B^*_{14} + A_{12}B^*_{24} + A_{13}B^*_{34} + A_{14}B^*_{44})e^{-iK\cdot r}]$$

$$C_{ij} = \sum_{k=1}^{N} A_{ik}B_{kj}$$

photoinduce index gratings

grating degeneracy

Reading

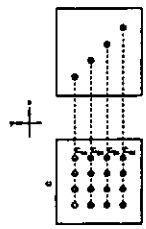

$$C_{14} = \sum_{k=1}^{4} A_{1k}B_{k4}$$

C. Gu *et al.*,Opt. Lett. 18,146(1993)

Nonlinear Optical Matrix Processor
– experimental result –

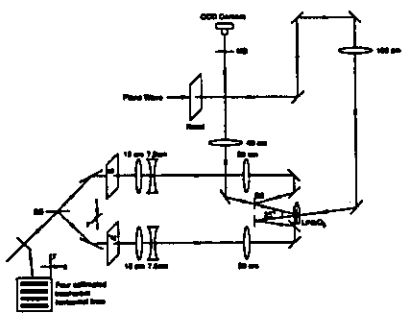

$$\underset{[A]}{\begin{bmatrix}1&0&1&0\\1&1&0&0\\1&0&1&1\\0&1&0&0\end{bmatrix}} \times \underset{[B]}{\begin{bmatrix}0&1&0&1\\1&0&1&0\\0&1&0&1\\0&1&0&1\end{bmatrix}} = \underset{[C]}{\begin{bmatrix}0&2&0&2\\1&1&1&1\\0&3&0&3\\1&0&1&0\end{bmatrix}}$$

Experimental result

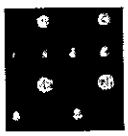

Processed result

$$\begin{bmatrix}0&2.0&0&2.1\\0.9&0.9&1.0&1.0\\0&3.0&0&3.0\\1.0&0&1.0&0\end{bmatrix}$$

• Response time determined by the total intensity
• 10^{12} operations per second with 1msec response time at $1W/cm^2$ total intensity for 1000×1000 matrices .

C. Gu *et al.*,Opt. Lett. 18,146(1993)

Volume Holographic Narrow-Band Optical Filter

Possible applications
- solar astronomy
- spectroscopy
- sensors
- optical communications

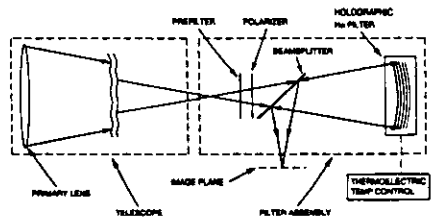

Optical setup for writing the volume grating for the holographic H-α (656.28nm) filter

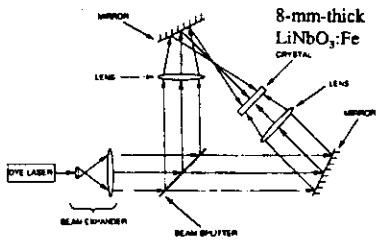

Peak reflectivity: > 50%
FWHM: 0.0125nm

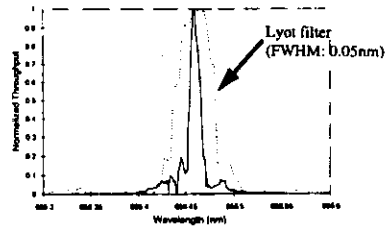

G.A.Rakuljic and V.Leyva.,Opt.Lett.18, 459(1993)

Applications of Phase Conjugation

Use of phase-conjugate waves
- **Imaging through scattering media**
- **Lensless imaging/focusing**
- **Fiber-dispersion compensation**
- **Laser power combining/injection locking**
- **Associative memories**
- **Optical interconnect**

Use as phase-conjugate interferometers
- **Image subtraction, addition and inversion**
- **Novelty filters**
- **Adaptive sensors/signal detection**
- **Double-exposure/time-average holographic interferometry**
- **Measurement of thin-film properties**

Holographic Time Gating for Imaging through Scattering Media

Photorefractive polymer
DHHADC-MPN:PVK:TNFDM:ECz
η=74%(59V/μm) at λ=830nm

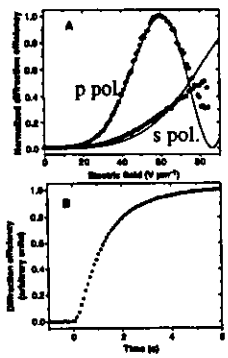

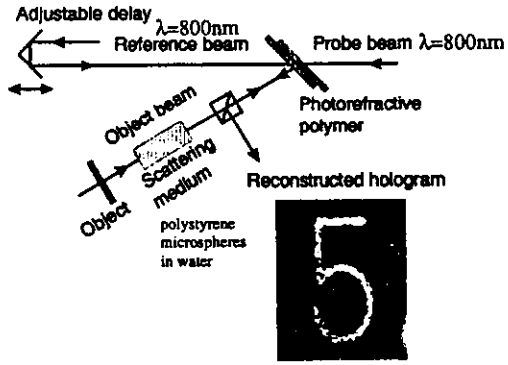

B.Kippelen *et al.*, Science 279, 54(1998)

Real-Time Image Addition, Subtraction and Inversion by Use of Phase Conjugate Mirror

Purpose

- compilation of composite images from separate inputs via *addition*
- difference detection, correction, and modification of images via *subtraction*
- deconvolution of images (e.g., deblurring of a distorted image) via *inversion*

$$I_{out} \propto |r_1|^2 \cos\theta \left| |T_1|^2 + \rho \tan\theta |T_2|^2 \right|$$

where

$\rho = \text{const.} \times (r_1 / r_2)$

•Subtaction : $\theta_{sub} = -\tan^{-1}(1/\rho)$

•Addition : $\theta_{add} = \tan^{-1}(1/\rho)$

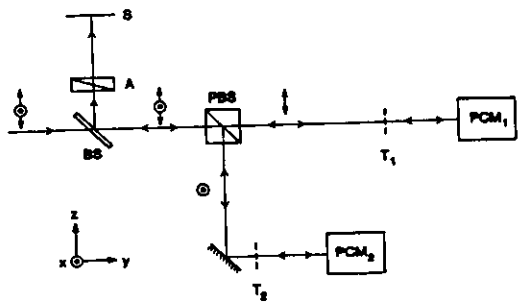

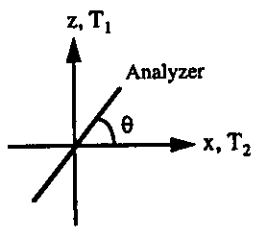

Experimental Setup

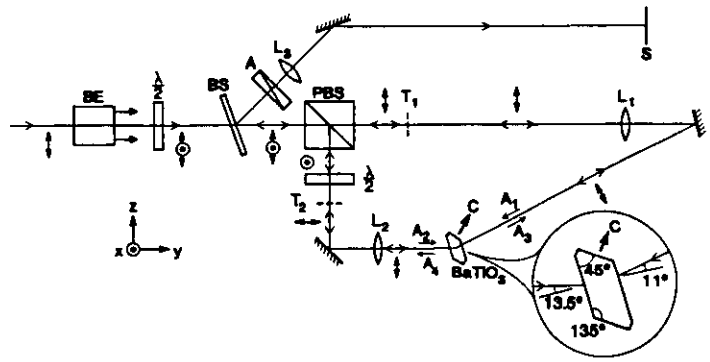

Y.Tomita et al., Appl.Phys.Lett. 52, 425(1988)

Experimental Results

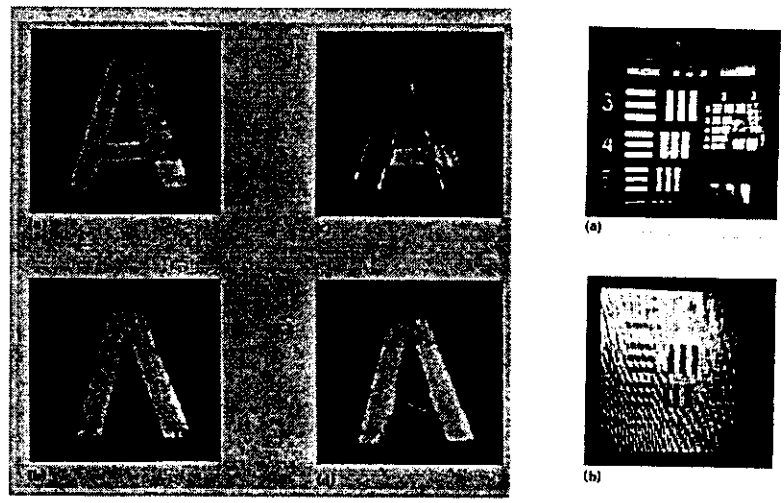

Y.Tomita et al., Appl.Phys.Lett. 52, 425(1988)

Phase Locking Lasers via Fiber-Coupled Phase-Conjugate Mirror

Efficient injection locking between lasers requirs optical mode matching

Use of mutually-pumped PCM

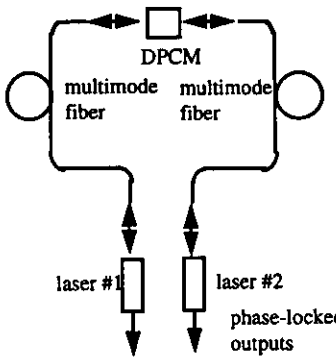

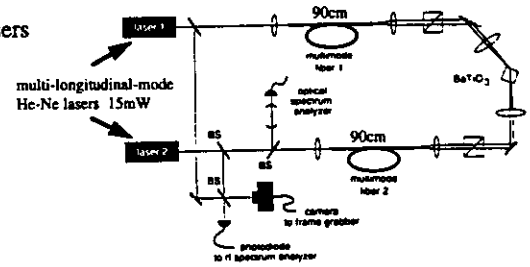

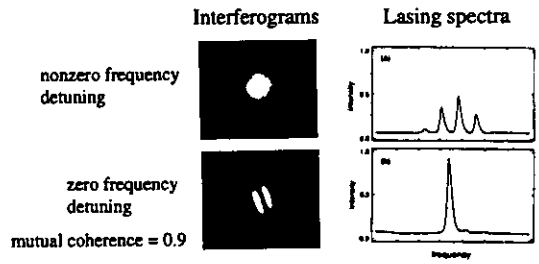

M.Grunelsen *et al.*, Opt. Commun. **100**, 173(1993)

Photorefractive Miltimode-to-Single-Mode Fiber-Optic Coupler

Technical difficulties in conventional methods
- very low coupling efficiency ≈ 1/(# of spatial modes)
- extremely sensitive to angular/lateral misalignment

Use of phase conjugation
- 2-to-3-orders-of-magnitude improvement in coupling efficiency
- self-adaptive system

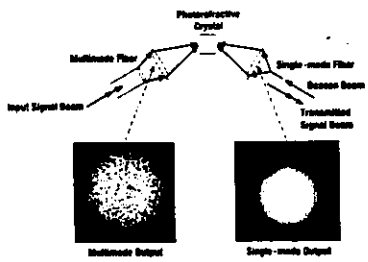

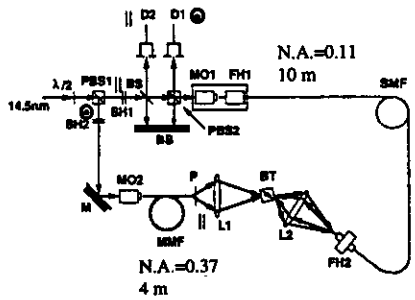

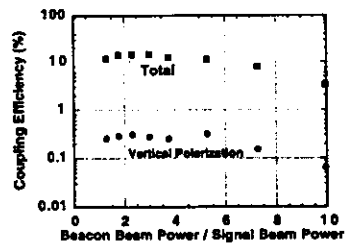

A. Chiou *et al.*, Opt. Lett. **10**, 1125 (1995)

Adaptive Spatially Injection-Locked Heterodyne Receiver

Requirement for coherent optical receivers in intersatellit links and optical radars
– High degree of spatial mode matching between the signal and local oscillator fields

Use of nonlinear optical phase conjugation instead of using traditional methods such as deformable mirrors or coherent arrays

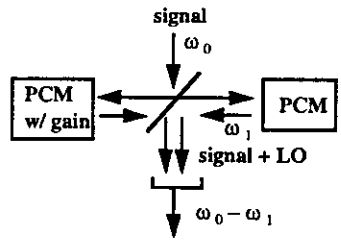

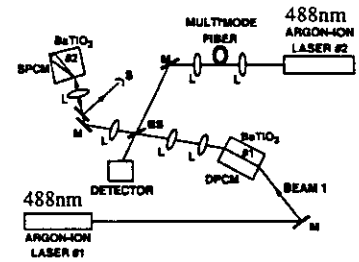

Heterodyne response

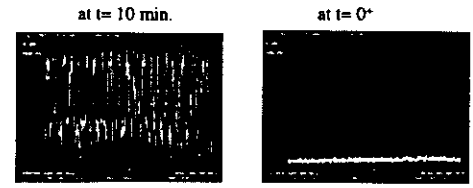

L.Adams and R.Bondurant, Opt. Lett. **18**, 226 (1993)